Chem Soc Rev

REVIEW ARTICLE

View Article Online
View Journal | View Issue

Cite this: *Chem. Soc. Rev.*, 2024, **53**, 3952

Received 30th December 2023

DOI: 10.1039/d3cs01165h

rsc.li/chem-soc-rev

Squaramide-based receptors in anion supramolecular chemistry: insights into anion binding, sensing, transport and extraction

Giacomo Picci,*[a] Riccardo Montis,*[b] Vito Lippolis[a] and Claudia Caltagirone*[a]

Over the last 15 years, squaramide-based receptors have attracted the attention of supramolecular chemists working in the field of anion recognition. Herein, we highlight examples of squaramide-based receptors that are able to bind, sense, extract and transport anions.

Introduction

One of the main strategies adopted by supramolecular chemists to bind anions is the development of synthetic receptors that are able to interact with anionic guests *via* the formation of hydrogen bonds (H-bonds). In this regard, the use of urea, thiourea, amide, and sulphonamide functional groups has been widely explored since the early 90's. More recently, the squaramide moiety has been added to the toolbox of H-bonding groups for the development of receptors for anion binding. The first report on squaric acid derivatives dates back to 1966 when Cohen and Cohen described the synthesis of alcoxy, hydroxy and amino derivatives starting from 1,2-dihydroxycyclobutenedione.[1] The success of the use of squaramides depends on some peculiar aspects related to the presence of a 4-membered ring in their molecular skeleton, such as its aromaticity according to the Hückel rule as the lone pair on the nitrogen atoms can delocalise on the cyclic structure and the aromatic character is increased when anion binding or deprotonation occurs as demonstrated by Frontera and Deya.[2] The aromaticity is related to the Brønsted acidity of the NH bonds which is an important aspect when comparing

[a] *Dipartimento di Scienze Chimiche e Geologiche, Università degli Studi di Cagliari, S.S. 554 Bivio per Sestu, Monserrato (CA) 09042, Italy. E-mail: gpicci@unica.it, lippolis@unica.it, ccaltagirone@unica.it*

[b] *Department of Pure and Applied Science, University of Urbino, Via della Stazione 4, Urbino I-61029, Italy. E-mail: riccardo.montis@uniurb.it*

Giacomo Picci

Giacomo Picci obtained his PhD degree in Chemical Science and Technology in 2020 under the supervision of Prof. Claudia Caltagirone and he is currently a non-tenured Assistant Professor at the Department of Chemical and Geological Science at the University of Cagliari. His research interests are focussed on supramolecular chemistry, and anion binding, sensing and transport and, more recently, on the development of supramolecular gels and their applications.

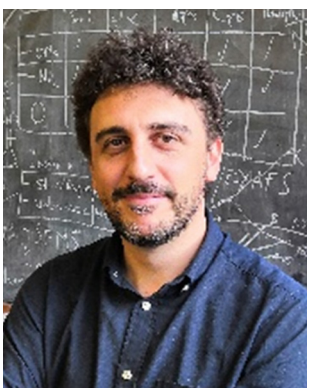

Riccardo Montis

Riccardo Montis graduated in Chemistry at the University of Cagliari in 2006, under the supervision of Prof. Vito Lippolis. In 2011, he received his PhD degree in Chemistry, under the supervision of Prof. Mike Hursthouse. After a number of postdoctoral positions in different Universities, such as the University of Southampton, Université libre de Bruxelles, University of Cagliari, Imperial College London and University of Manchester, in 2021, he joined the University of Urbino "Carlo Bo" as an Assistant Professor. His research interests cover different aspects of supramolecular chemistry, including the design of receptors for anion binding and crystal engineering.

this class of compounds with analogous croconamides and deltamides.[3] Squaramides are also characterised by their ability to act both as H-bond donors (*via* the NH groups) and H-bond acceptors (*via* the carbonyl groups) and this aspect is particularly relevant for applications in organocatalysis.[4] Several reports have demonstrated how the rigidity of the 4-membered ring, the directionality of the NH bonds, and the bond angles make squaramides better candidates as receptors for anion binding compared to analogous ureas.[5,6]

For all these reasons, as well as for synthetic accessibility, squaramides have started to be widely used as receptors for anion binding, sensing, extraction, transport and, very recently, for the development of different anion-responsive materials. Some efforts have been directed towards exploring polymers,[7,8] nanomaterials,[9] and soft materials.[10] As an example, Wezenberg and co-workers recently described that polymeric gels containing a squaramide crosslinker were able to swell and bend in the presence of different concentrations of various anions.[11]

Although the topic has already been the subject of previous reviews covering different aspects of application of squaramides in supramolecular chemistry,[12–14] herein we will highlight examples of the use of squaramides for anion binding, extraction, sensing and transmembrane transport with the purpose of providing some inputs for the future of this very active field of research.

Anion binding

The first use of squaramide derivatives for carboxylate binding has been reported by Costa, Ballester and co-workers in 1998.[15] In this seminal paper, they described the series of mono squaramides **1–4**, symmetric and non-symmetric, bearing neutral or charged substituents (Fig. 1). When titrated with tetramethylammonium acetate in DMSO-d_6 or in a mixture of DMSO-d_6/10%D_2O by means of ^{1}H-NMR titrations, these receptors showed a moderate affinity for this anion forming adducts with 1 : 1 stoichiometry with the highest association constant measured for squaramide **4** in DMSO-d_6 (K_{ass} = 14 200 ± 3200 M^{-1}). As expected, the presence of the positively charged trimethylammonium group on one of the pendant arms of **4** improves the anion binding properties of this receptor.

Authors showed that an efficient binding of dicarboxylates could be achieved with bis-squaramides **5–9** (Fig. 1). For example, squaramide **7** bearing two benzylic substituents showed association constants for the formation of the 1 : 1 adduct with glutarate [as its tetrabutylammonium (TBA) salt] in DMSO-d_6/10%D_2O of 1400 ± 200 M^{-1} and in DMSO-d_6/15%D_2O of 150 ± 40 M^{-1} while in DMSO-d_6 the association constant was too high to be measured by ^{1}H-NMR spectroscopy (K_{ass} > 10^4 M^{-1}). The charged bis-squaramide **9** was able to bind glutarate in a very hydrophilic medium such as CD_3CN/30%H_2O with an association constant of 560 ± 50 M^{-1} demonstrating the efficiency of the squaramide NHs to act as H-bond donor groups even in a very competitive solvent medium. Finally, the authors reported the ability of receptors **10** and **11** characterised by a pseudo C_3 symmetry to bind tricarboxylates (Fig. 2). Indeed, tris-squaramide **11** was able to bind trimesoate and *cis*-cyclohexentricarboxylate (both as their TBA salts) with association constants for the formation of the corresponding 1 : 1 adducts in DMSO-d_6/10%D_2O of 3900 ± 400 M^{-1} and 7700 ± 1300 M^{-1}, respectively.

Costa's group also gave insight into the thermodynamic aspects behind the carboxylate binding by the mono and bis-squaramides described above, showing by ITC that in solvents

Vito Lippolis

Vito Lippolis graduated in Chemistry in 1991 at the University of Pisa, Italy, and in the same year he gained a diploma in Chemistry at the "Scuola Normale Superiore" of Pisa. In 2000, he received his PhD degree from the University of Nottingham (UK), under the supervision of Professor Martin Schröder. In 2001, he was appointed as the Chair of Inorganic Chemistry at the University of Cagliari, Italy. His research activity mainly concerns the development of molecular sensors and ionophores for heavy metal ions and anions and fluorescent materials, the study of the interaction between chalcogen donor molecules and halogens and inter-halogens, and the synthesis and study of new metaldithiolene complexes for applications in the fields of laser technology and semiconductors. He has published over 360 publications.

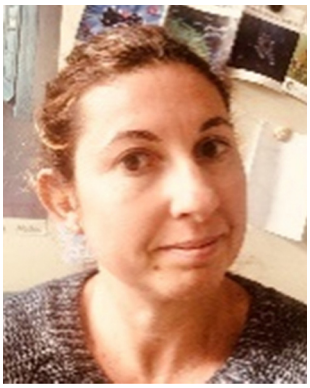

Claudia Caltagirone

Claudia Caltagirone is an Associate Professor in Inorganic Chemistry at the University of Cagliari. She received her PhD degree in Chemical Science in 2006 under the supervision of Prof. Vito Lippolis. She spent two years in Southampton in Philip Gale's group from 2006 to 2008. Claudia's research interests in Supramolecular Chemistry are focussed on the design, synthesis and characterisation of molecular chemosensors for anion and cation recognition and transport and on the design of novel supramolecular architectures based on non-covalent interactions. She is a member of the Italian Supramolecular Chemistry Steering Committee and Co-chair of the Women in Supramolecular Chemistry (WISC) Network.

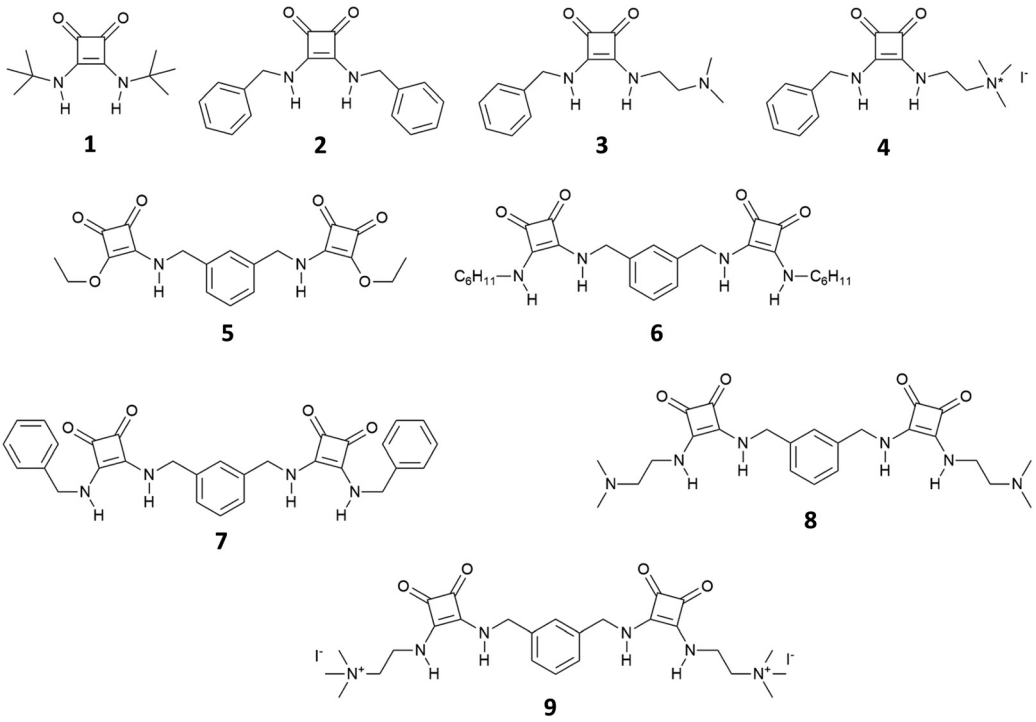

Fig. 1 Receptors **1–9** developed by Costa, Ballester and co-workers for carboxylate and dicarboxylate binding.

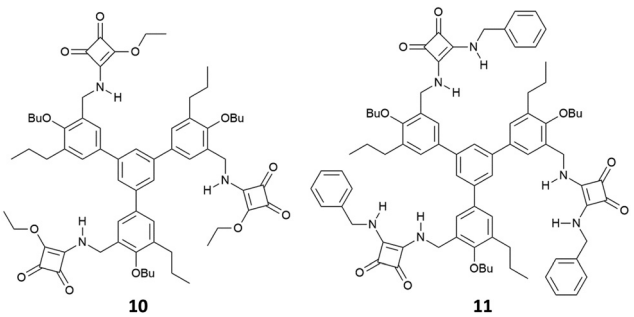

Fig. 2 Receptors **10–11** developed by Costa, and co-workers for tricarboxylate binding.

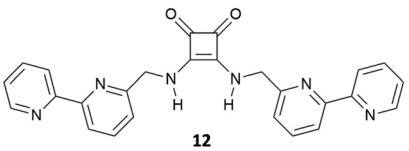

Fig. 3 Receptor **12** synthesised by Al-Sayah and Branda.

such as $CHCl_3$ or DMSO the formation of the adducts between squaramide derivatives (especially in the case of those bearing positively charged ammonium groups) and carboxylates anions are driven by the formation of H-bonds and electrostatic interactions, and the process is overall exothermic. In polar solvents, such as CH_3OH, the interactions still occur but the process is endothermic and entropically driven by the reorganization of solvent molecules during the binding event.[16]

Al-Sayah and Branda have studied the carboxylate binding properties of squaramide **12** (Fig. 3) and compared them with those of the analogous thiourea.[17] Upon ^{1}H-NMR titration of **12** with TBAAcO in $CD_3CN/CDCl_3$ (1 : 1 v/v), an association constant of 7390 M^{-1} was calculated for the formation of the 1 : 1 adduct, while a lower association constant (K_{ass} = 5790 M^{-1}) for the formation of the acetate adduct with the analogous thiourea was determined. Authors also performed calorimetric titration studies in $CH_3CN/CHCl_3$ (1 : 1 v/v) demonstrating that the binding event is both enthalpically and enthropically driven with a ΔH of −2209 cal mol^{-1} and a ΔS of 10.3 cal mol^{-1} K^{-1}.

Very recently, Elmes and co-workers have reported on a family of symmetric squaramides (**13–15**) functionalised with naphthalimide groups differing for the length of the aliphatic chain between the squaramide core and the substituents (Fig. 4).[18] As shown by the SEM image reported in Fig. 4(A), squaramide **13** undergoes molecular self-assembly/aggregation giving rise to some sort of pine cone structures. A similar behaviour was observed in the cases of **14** and **15**. The aggregation behaviour was further confirmed by ^{1}H-NMR studies in DMSO-d_6 at variable temperatures (Fig. 4(B)) which demonstrated that at 298 K the signals assigned to the squaramide NHs and the naphthalimide CHs appeared broad while they became sharper and resolved well by increasing the temperature up to 358 K. The aggregation/disaggregation process was reversible as the peaks became broad again by cooling down back to 298 K. The three squaramide derivatives were able to selectively bind AcO^- (as its TBA salt) in DMSO with low association constants (K_{ass} = 422 ± 11.9% M^{-1} for the 1 : 1 adduct formation calculated with receptor **13** at 273 K). This is

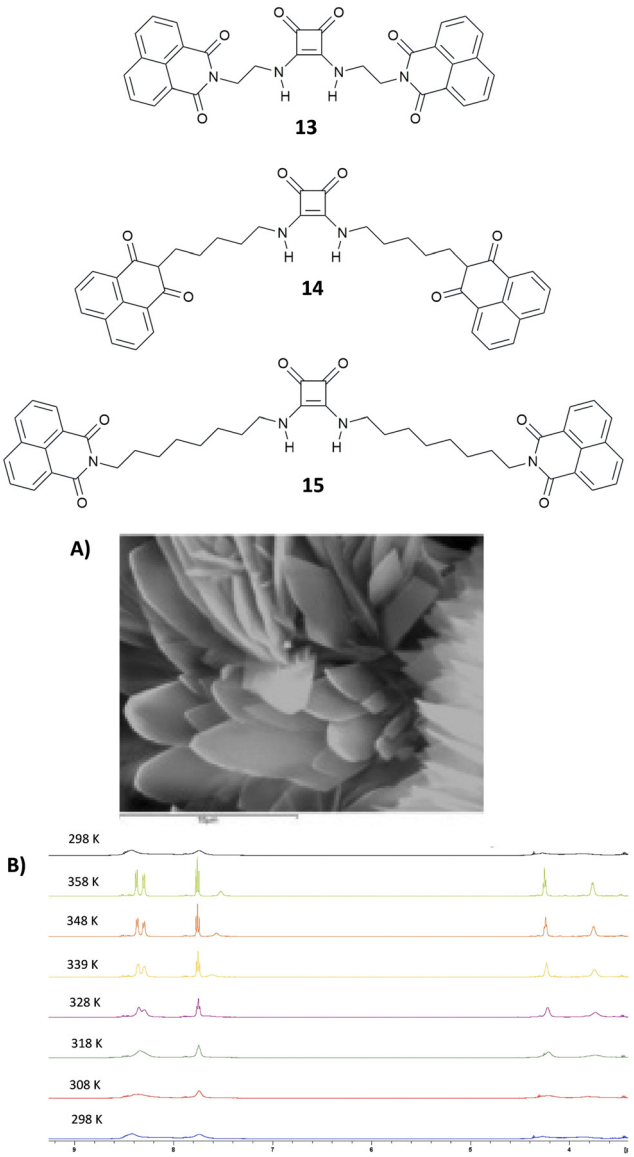

Fig. 4 Squaramides **13–15** reported by Elmes and co-workers. SEM image of **13**, and the scale bar is 10 μm (A). ^{1}H-NMR spectrum of **13** (5.0×10^{-3} M) recorded at variable temperatures in DMSO-d_6 (B). Reproduced with permission from ref. 18. Copyright Elsevier 2022.

probably due to a competition between the self-aggregation of the free receptors and the formation of the adducts. The authors demonstrated that the length of the chain in the design of the receptors does not have any effect as they all showed a similar behaviour.

Recently, a series of squaramides able to bind non-steroidal anti-inflamatory drugs (NSAIDs) ketoprofen and naproxen as their sodium salts have been reported (Fig. 5).[19,20] The macrocyclic systems **16** and **17** have been found to be able to bind ketoprofen in its anionic form in a 1 : 1 stoichiometry in CH_3CN/DMSO solution (1 : 1 v/v) with association constants of $K_{ass} = 9.4 \times 10^4 \pm 0.6\%$ and $K_{ass} = 8.3 \times 10^4$ $M^{-1} \pm 1\%$, respectively. Receptors **19–24** were employed successfully for developing ion selective electrodes (ISEs) able to discriminate

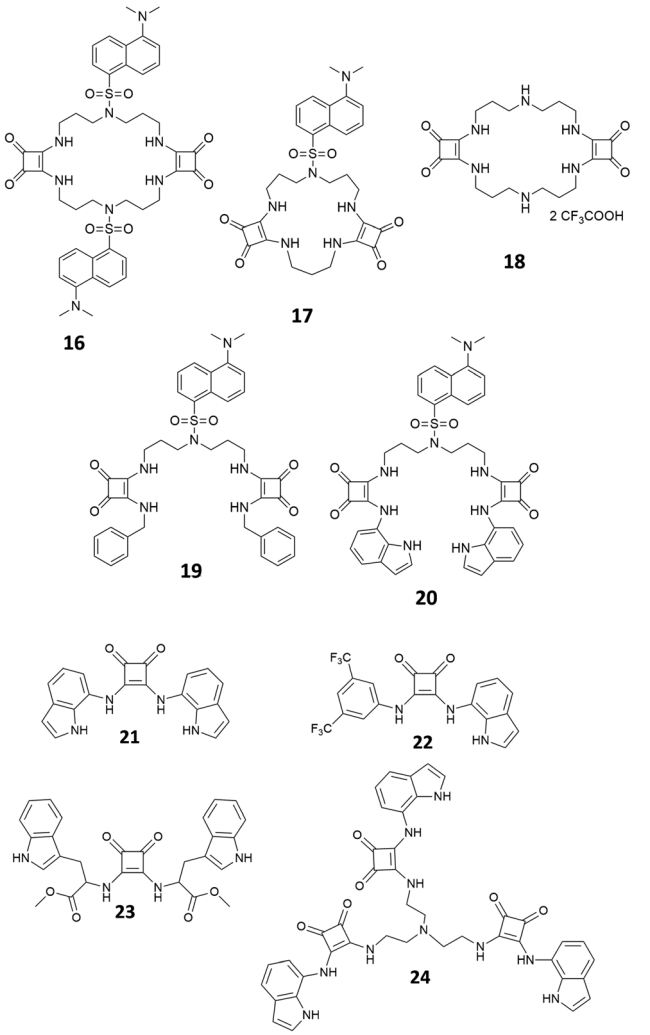

Fig. 5 Squaramides for naproxen and ketoprofen binding in their anionic forms.

ketoprofen and naproxen in their anionic forms in real samples.

Few examples of squaramide receptors for selective phosphate binding have been reported in the literature, to the best of our knowledge. Elmes and co-workers have described two novel self-associating amphiphilic (SSA) squaramides **25** and **26** (Fig. 6), which are able to bind anions in DMSO, while in a more

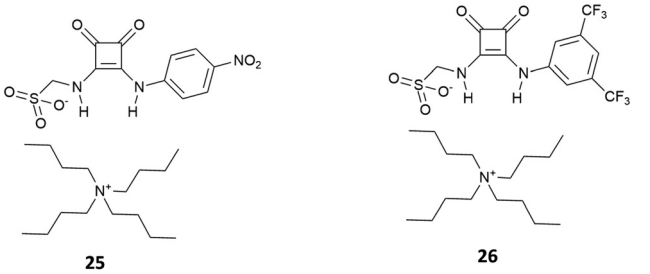

Fig. 6 SSA squaramides that are able to act as colorimetric sensors for $H_2PO_4^-$.

competitive solvent medium such as DMSO/H_2O (1 : 1 v/v) the deprotonation event caused by $H_2PO_4^-$ (as its TBA salt) on receptor **16** is able to cause a colour change of the solution.[21]

A well-known strategy in anion supramolecular chemistry is the exploitation of vacant coordination positions on a metal centre to bind anions.[22] This strategy was successfully used by Delgado and co-workers to bind phosphate anions in water. Squaramide **27**, bearing dipicolylamine (dpa) and ethylpiperazine substituents, forms stable copper(II) complexes in water with different degrees of protonation depending on the pH. In particular, the binucluear complexes $[Cu_2\mathbf{27}H_{-i}]^{(4-i)+}$ in which the metal centres are in a distorted octahedral environment determined by the nitrogens of the dpa/ethylpiperazine moieties, a nitrogen atom and an oxygen atom of the squaramide unit (Fig. 7(A) for the $[Cu_2\mathbf{27}H_{-1}]^{3+}$ calculated structure) and two H_2O molecules. At physiological pH values, the dinuclear complexes $[Cu_2\mathbf{27}H_{-i}]^{(4-i)+}$ bind selectively ATP^{4-} over ADP^{3-}, AMP^{2-}, aminoethylphosphate ($Haep^-$) and phenylphosphate ($PhPO_4^{2-}$), with significant interference of hydrogenpyrophosphate ($HPPi^{3-}$) with very high association constants. DFT calculations, as shown in Fig. 7(B) and (C), revealed that in the presence of $HPPi^{3-}$ and ATP^{4-}, the aqua ligands bound to the metal centres are replaced by the oxygen atoms of the anion guests and a further H-bond interaction between the hydroxyl group of the ribose unit and the squaramide oxygen atoms in the case of ATP^{4-}, which stabilize the complexes.

The cryptand-like receptor **28** (Fig. 8) was reported by Fusi, Micheloni and co-workers.[23] It consists of two separate binding sites: a Me_2[12]aneN_4 polyaza macrocyclic unit suitable for cation binding bridged by two squaramide units suitable for anion binding.

Macrocycle **28** was found to be selective for $H_2PO_4^-$ over SO_4^{2-} and $H_2P_2O_7^{2-}$ (the log K_{ass} values for SO_4^{2-}, $H_2PO_4^-$, and $H_2P_2O_7^{2-}$ are 2.96, 4.04, and 2.56, respectively) as determined by potentiometric titrations in 0.15 M $NaClO_4$ aqueous solution. Potentiometric studies also highlighted that the selectivity for $H_2PO_4^-$ was maintained in the pH range of 4.0–10.5 with a peak of selectivity at pH 7.4.

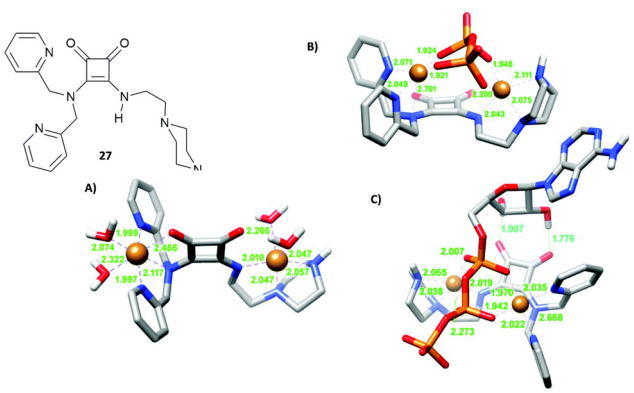

Fig. 7 Squaramide **27** reported by Delgado and co-workers and its dinuclear copper(II) complex $[Cu_2\mathbf{27}H_{-1}]^{3+}$ (A), complex $[Cu_2\mathbf{27}H_{-1}(PPi)]^-$ (B), complex $[Cu_2\mathbf{27}H_{-1}(ATP)]^-$ optimised by DFT calculations (C). Adapted with permission from ref. 22. Copyright RSC 2019.

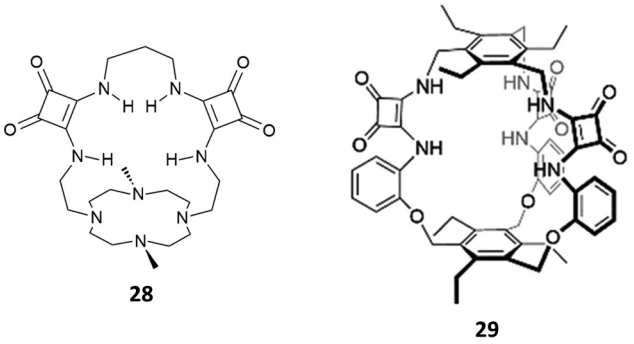

Fig. 8 Cryptand-like and cage-like squaramide-containing receptors **28** and **29** for dihydrogenphosphate binding.

Very recently, Kim and Yang reported the excellent binding behaviour in solution and in the solid state of the cage-like squaramide receptor **29** (Fig. 8).[24] The anion binding properties of **29** in the presence of a set of anions as their TBA salts (fluoride, chloride, bromide, iodide, hydrogensulfate, sulfate, hydrogenpyrophosphate, and dihydrogenphosphate or triethylammonium hydrogencarbonate) were studied in DMSO-d_6/10%H_2O by means of ^{1}H-NMR titrations. A downfield shift of the signals attributed to the squaramide NHs was observed upon the addition of the anions. By fitting the titration data using a 1 : 1 binding model, an association constant of K_{ass} = (6.57 ± 1.12) × 10^2 M^{-1} was determined for the formation of the adduct of **29** with $H_2PO_4^-$. The formation of the 1 : 1 adduct was confirmed by a Job plot experiment in solution and by SCXRD analysis in the solid state. Single crystals were grown by slow evaporation of a $CHCl_3$/CH_3OH solution of **29** in the presence of an excess of $TBAH_2PO_4$. As shown in Fig. 9, the anion is bound to the squaramide NHs *via* four H-bonds. The anion also forms H-bonds with CH_3OH molecules and the carbonyl groups of the squaramide moieties of an adjacent receptor molecule.

One of the most targeted anions in the development of artificial receptors for anionic systems is sulfate, SO_4^{2-},[25,26] which is involved in numerous biological, environmental, and chemical processes.[27–29] This is not an easy task considering the tetrahedral shape of this anion, its charge density and high hydrophilicity (ΔG_h = −1080 kJ mol^{-1}),[30] which require

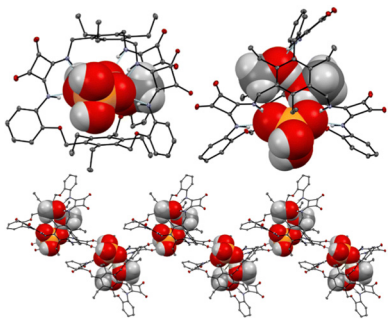

Fig. 9 Views of the single X-ray crystal structure of the 1 : 1 adduct of **29** with $TBAH_2PO_4$. Reproduced from ref. 24. Copyright RSC 2023.

an accurate choice of building blocks, functional groups and related spatial disposition in the structure of the abiotic receptors in order to maximize non-covalent interactions *via* topological complementarity. In fact, SO_4^{2-}, binding proteins (SBPs), which are involved in the high selective binding and active transport of this anion into bacteria cells, feature binding sites located in hydrophobic pockets far from the protein surfaces where the SO_4^{2-} anion can be bound in a dehydrated form and completely shielded from the solvent.[31] Furthermore, a precise arrangement in the binding sites of selected amino-acids with appropriately oriented H-bonding donor groups allows the exact encapsulation and efficient binding (an association constant of about 10^6 M^{-1} in H_2O at pH 5–9)[32] and recognition of the tetrahedral SO_4^{2-} anion *via* the formation of seven H-bonds.

Inspired by nature, many researchers have proposed macrocyclic,[33] interlocked,[34] and tripodal[35] scaffolds for selective SO_4^{2-} receptors, featuring various H-bond donor binding sites, among which also squaramide moieties.

In 2013, considering the results achieved with the well-known tren-based tris-(thio)urea receptors for anion binding,[36,37] Jiang, Lin and co-workers reported the tripodal receptors **30–32** (Fig. 10) and investigated by ^{1}H-NMR their binding properties towards inorganic anions as TBA salts in DMSO-d_6.[38]

The results indicated that receptors **30–32** show strong binding affinities or acid–base interactions with Cl^-, SO_4^{2-}, HSO_4^-, $H_2PO_4^-$, and AcO^- (Cl^- and $H_2PO_4^-$ provoked deprotonation of **31** and **32**) with a preference for SO_4^{2-} [K_{ass}: 4.75 (**30**), 4.95 (**31**), and 4.87 M^{-1} (**32**)] followed by the other anions in the order $H_2PO_4^-$ [K_{ass}: 4.14 (**30**) M^{-1}], HSO_4^- [K_{ass}: 3.65 (**30**), 3.78 (**31**), and 3.65 M^{-1} (**32**)], AcO^- [K_{ass}: 2.82 M^{-1} (**30**)], and Cl^- [K_{ass}: 2.58 (**30**), 2.61 (**31**), and 2.65 M^{-1} (**32**)] and a fine modulation exerted by substituents present on the phenyl groups. In any case, these receptors showed a binding affinity for SO_4^{2-} higher than those observed for urea-based tripodal systems.[36,37] Interestingly, all evidences (including Job plots and DOSY NMR experiments) suggested the formation of a 1 : 1

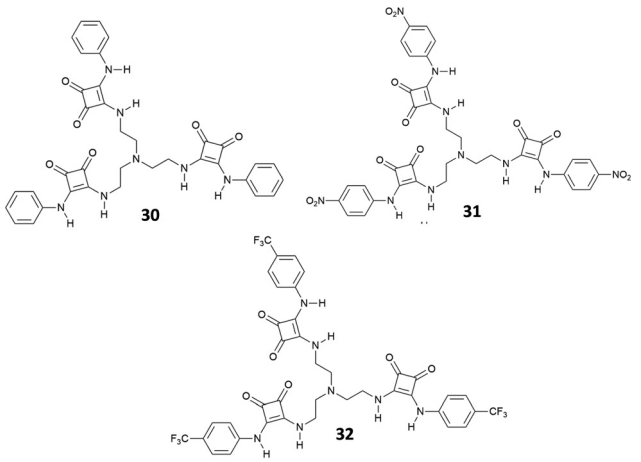

Fig. 10 Molecular structures of the tren-based tris(squaramide) receptors **30–32**.

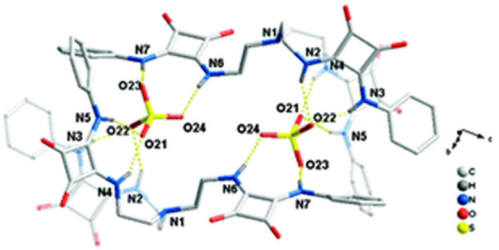

Fig. 11 Molecular structure of the 2 : 2 adduct $[[\mathbf{30}(SO_4)]_2]^{2-}$ in $[\mathbf{30}(SO_4)]_2(TBA)_2$. Reproduced with permission from ref. 38. Copyright RSC 2013.

adduct in solution between **30** and SO_4^{2-}, despite in the solid state the 2 : 2 $[\mathbf{30}(SO_4)]_2(TBA)_2$ dimeric adduct was isolated and structurally characterized (Fig. 11). Each SO_4^{2-} anion in the dimer is coordinated by the NH protons of the squaramide units from two arms of **30** and by the squaramide moiety belonging to a symmetry related receptor unit.

The same authors successfully employed these receptors as anionophores in the preparation of ISEs for sulfate recognition.[39] In particular, the membrane prepared incorporating receptor **31** showed a Nernstian slope of −30.2 mV with a linear range from 1 μM to 100 mM sulfate concentration and was employed for the quantification of sulfate in cell lysates and drinking water. Jolliffe and co-workers have reported a series of neutral macrocyclic receptors of different ring size cavities, preorganization for SO_4^{2-} binding, and solubility in aqueous media, featuring two or three squaramide moieties in their structures and two or three benzene (Fig. 12) or pyridine spacer units (Fig. 13).[40,41]

Receptors **33–36** contain alternating aryl and squaramide units (Fig. 12), and they do not feature triethyleneglycol monomethyl pendants *via* ester or amide linkages for **37–42**. Unfortunately, despite clear evidences for the ability to bind strongly SO_4^{2-}, due to the low solubility even in DMSO-d_6, and the complexity of the ^{1}H-NMR spectra, quantitative anion binding studies were not possible for **35** and **36**.[42] In the case of the more soluble **33** and **34**, these studies were performed in DMSO-d_6/0.5%H_2O by titration with the TBA salts of the anions

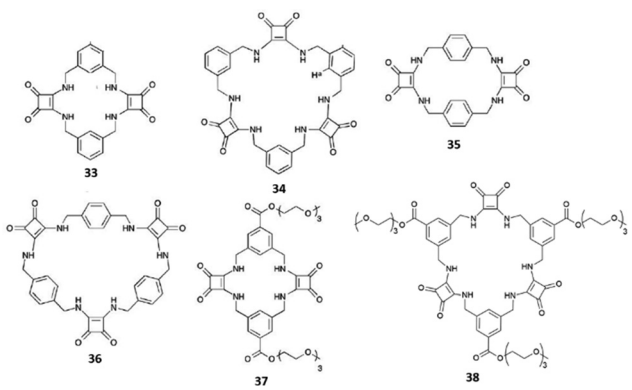

Fig. 12 Cyclic squaramide-based receptors featuring aryl spacers and in the cases of **37** and **38** also triethylene glycol monomethyl pendants *via* ester linkages.

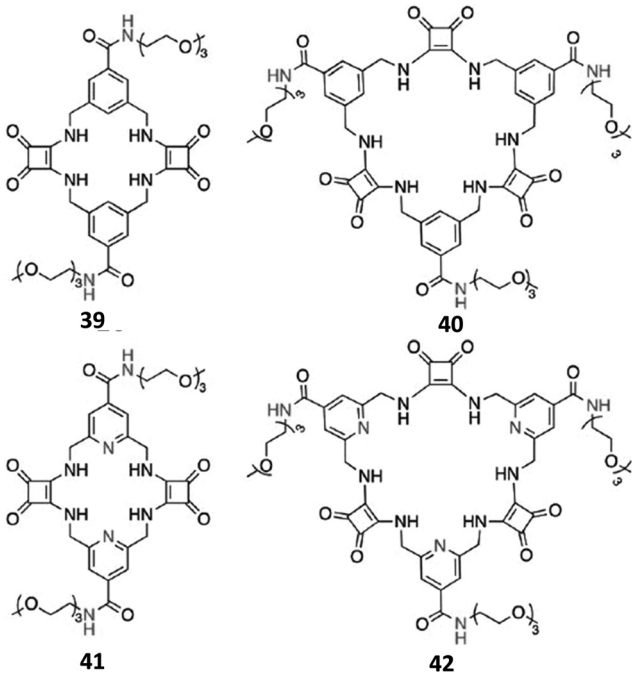

Fig. 13 Cyclic squaramide-based receptors **39–42** featuring benzene or pyridine spacers and triethylene glycol monomethyl pendants *via* amide linkages.

SO_4^{2-}, $H_2PO_4^-$, AcO^-, and Cl^-, for which preliminary results indicated a strong interaction with the two receptors in DMSO-d_6 (in the presence of F^-, deprotonation of the NH protons was observed for **33** and **34** in DMSO-d_6).[42] In this medium, both **33** and **34** were found to bind SO_4^{2-} with association constants (K_{ass}) higher than 10^4 M^{-1} for the formation of 1 : 1 adducts. However, significant differences were observed for the measured binding constants with the other anions with the highest selectivity for the SO_4^{2-} observed in the case of **34** [K_{ass}: $>10^4$ (SO_4^{2-}), $>10^4$ ($H_2PO_4^-$), 7530 (AcO^-), and 28 M^{-1} (Cl^-) for **33**; $>10^4$ (SO_4^{2-}), 409 ($H_2PO_4^-$), 776 (AcO^-), and 144 M^{-1} (Cl^-) for **34**].[42] ^{1}H-NMR spectra indicated the involvement of both squaramide NH protons and aromatic CHs sitting between the two benzene ring substituents in SO_4^{2-} and $H_2PO_4^-$ binding by both **33** and **34**. For the other two anions, only the NH protons appeared to be involved in the binding. A clear picture of the binding mode of **33** with SO_4^{2-} comes from the X-ray crystal structure of the complex $[\mathbf{33}(SO_4)](TBA)_2{\cdot}2H_2O$.[42] In the complex anion $[\mathbf{33}(SO_4)]^{2-}$, the receptor adopts a bowl-like conformation, reminiscent of a calixarene in the cone conformation, with NH protons from both squaramide units and the two aromatic CH protons (one from each benzene ring) pointing towards the macrocyclic cavity (Fig. 14). In this conformation, the prevailing binding mode of the SO_4^{2-} anion by the receptor involves the formation of NH$\cdots$O H-bonds between each of the four amide protons and three of the anion oxygens as shown in Fig. 14(A) and (B). The free coordination hemisphere of SO_4^{2-} is nestled among the butyl chains of the TBA^+ counter cations. Interestingly, the optimized geometry of the anion $[\mathbf{33}(AcO)]^-$ features the anion bound to the four NH protons, but the aromatic CH protons sitting between the two benzene ring substituents point away from the anion binding site and the conformation assumed by the receptor is reminiscent more of that observed for a 1,3-alternate calixarene.[42]

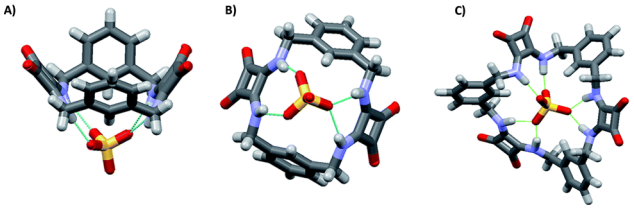

Fig. 14 Two different views of the structure of the complex anion $[\mathbf{33}(SO_4)]^{2-}$ with the receptor in the dominant binding mode (A) and (B). The optimized model of the complex anion $[\mathbf{34}(SO_4)]^{2-}$ (C). Reproduced with permission from ref. 42. Copyright RSC 2016.

The higher selectivity of **34** towards the SO_4^{2-} anion is supported by the optimized structure of the complex anion $[\mathbf{34}(SO_4)]^{2-}$ (Fig. 14(C)). The SO_4^{2-} anion sits inside the macrocyclic cavity with all four oxygens engaging H-bonds with the squaramide NH protons, all six of them being involved. Furthermore, all three benzene rings have one proton pointing towards the SO_4^{2-} anion, thus suggesting the involvement of them in additional stabilizing interactions, which would contribute to the high affinity and selectivity of **34** for SO_4^{2-}.

The introduction in **37** and **38** of triethylene glycol monomethyl pendants *via* ester linkages allowed anion binding in H_2O/DMSO-d_6 (1 : 2 v/v) to be studied by ^{1}H-NMR. In this more competitive solvent mixture, a remarkable decrease of the association constant was observed for **37** [K_{ass}: 1820 M^{-1} (SO_4^{2-})] compared to **33** [K_{ass}: $>10^4$ M^{-1} (SO_4^{2-})] in the formation of the 1 : 1 adduct. However, receptor **38** still showed a high affinity for SO_4^{2-} [K_{ass}: $>10^4$ M^{-1}]. This was attributed not only to the presence in **38** of an additional squaramide and aromatic CH binding sites, but mainly to the perfect match of the size of the anion to the cavity of the receptor, which allows the former to be protected from the interactions with solvent molecules in a sort of hydrophobic cavity. In H_2O/DMSO-d_6 (1 : 2 v/v), **38** showed also great selectivity for SO_4^{2-} in comparison with other tetrahedral anions such as phosphate species (K_{ass}: 16 M^{-1} at pH 7 in the presence of both $H_2PO_4^-$ and HPO_4^{2-}), SeO_4^{2-} (K_{ass}: 1900 M^{-1}), CrO_4^{2-} (K_{ass}: 165 M^{-1}), and ClO_4^{2-} (K_{ass}: too low to be determined). ^{1}H-NMR titrations of **38** with SO_4^{2-} and phosphate species in H_2O/DMSO-d_6 (1 : 2 v/v) were also performed at pH 9.1 (tris buffer) at which the predominant phosphate species is HPO_4^{2-}; under these conditions, the K_{ass} values observed for the two anions were 2045 and 13 M^{-1}, respectively. A higher affinity of **38** for sulfate than other anions was also confirmed in aqueous mixtures [H_2O/DMSO-d_6 (1 : 1 v/v)] mimicking the anion composition of plasma (measurements made at pH 7.4) and nuclear waste (pH 3.2).

In order to further increase the solubility in aqueous DMSO mixtures with a higher water content, and the SO_4^{2-} binding affinity and selectivity over a wide pH range, Joliffe and coworkers also synthesised the receptors **39–42** (Fig. 13), which

are structural analogues of **37** and **38**, but feature amide linkages instead of ester ones for decorating the macrocyclic structures with the solubilizing triethyleneglycol chains, and pyridines instead of benzene spacers (**41** and **42**).[40] As expected, receptors **40** and **42** (featuring three squaramide units in their structures) displayed higher affinities than analogues **39** and **41** (featuring two squaramide units in their structures), in both H_2O/DMSO-d_6 (1 : 9 v/v) and H_2O/DMSO-d_6 (1 : 2 v/v) at pH 7, as already observed for **38** with respect to **37** (the low solubility of **41** in the latter solvent mixture prevented an evaluation of its SO_4^{2-} binding affinity in this medium), with K_{ass} values for the 1 : 1 adduct formation higher than 10^4 M^{-1}. While the replacement of ester linkages by amide ones resulted in a little impact on the SO_4^{2-} binding ability, the replacement of benzene spacers with pyridine ones revealed to be a winning strategy. In fact, due the higher solubility of **40** and **42** in comparison to that of **34**, ^{1}H-NMR binding studies were performed for these two receptors also in DMSO-d_6/H_2O (1 : 1 v/v) at pH 7. In this very competitive medium, **42** resulted to bind SO_4^{2-} about three times more strongly than **40** (K_{ass}: 4870 and 1340 M^{-1} for **42** and **40**, respectively), and this selectivity was maintained even in DMSO-d_6/H_2O (1 : 2 v/v) (K_{ass}: 480 and 130 for **42** and **40**, respectively). In agreement with DFT calculations, this behaviour was attributed to a greater preorganization of **42** to SO_4^{2-} binding due to intramolecular H-bonds between the pyridine N atoms and the NH protons with the free ligand that presents in its more stable conformation all squaramide protons already pointing towards the centre of the ring cavity. In contrast, **40** would undergo a significant conformational change for SO_4^{2-} binding through all six NH protons (Fig. 15).

Significantly, in DMSO-d_6/H_2O (1 : 1 v/v), binding of the anions AcO^-, NO_3^-, Cl^-, HCO_3^- and $H_2PO_4^-$ to **42** was negligible as no changes in the ^{1}H-NMR spectrum of the receptor was observed upon addition of 5 equiv. of these anions.

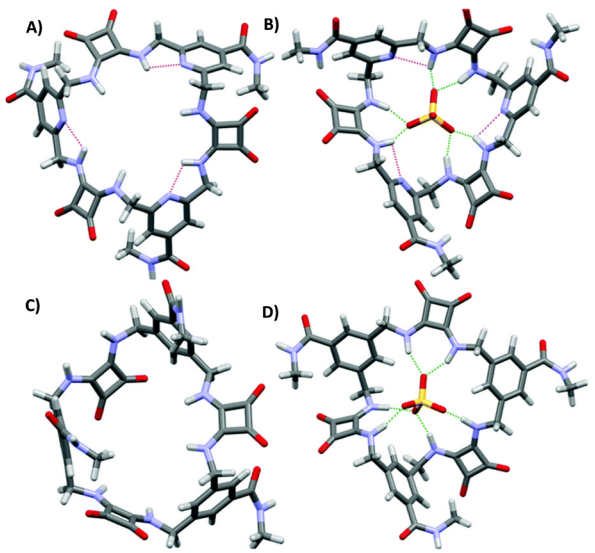

Fig. 15 Optimized structures of **42** (A), **40** (C), [**42**$(SO_4)]^{2-}$ (B), and [**40**$(SO_4)]^{2-}$ (D). Reproduced with permission from ref. 41. Copyright RSC 2019.

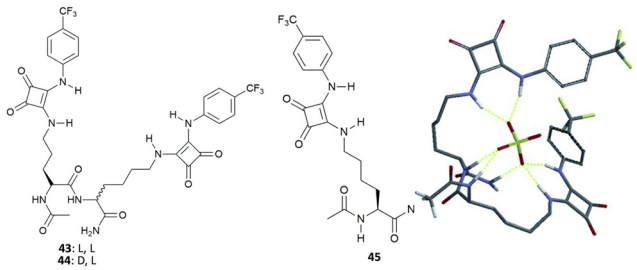

Fig. 16 Molecular structures of dipeptides **43–45** featuring squaramide functionalized side chains and the modelled structure of the adduct [**43**$(SO_4)]^{2-}$ showing the possible H-bond patterns responsible for the high binding affinity of **43** towards SO_4^{2-} in very competitive solvent mixtures. Reproduced with permission from ref. 43. Copyright Wiley 2014.

Furthermore, in this medium, **42** exhibited a binding selectivity for SO_4^{2-} over SeO_4^{2-} and CrO_4^{2-} with a selectivity index for the latter ($K_{ass(sulfate)}/K_{ass(chromate)}$ = 483) much better than that observed for **38** under the same experimental conditions. Compared to **38**, the SO_4^{2-} binding performances of **42** resulted significantly increased also in aqueous mixtures [DMSO-d_6/H_2O (1 : 1 v/v)] mimicking the anion composition of plasma (measurements made at pH 7.4, K_{ass}: 2490 M^{-1}) and nuclear waste (pH 3.2, K_{ass}: 4870 M^{-1}) in the presence of competing anions, and under conditions of pH 14 (K_{ass}: 610 M^{-1}) in which the receptor resulted stable for 5 hours.

Neutral dipeptides **43** and **44** bearing squaramide functionalised side chains have been reported by Joliffe and co-workers as efficient SO_4^{2-} receptors in mixtures of DMSO and H_2O (Fig. 16).[43]

Due to the large association constant of these receptors with SO_4^{2-} in DMSO-d_6 containing 0.5% of water (v/v) (strong binding is suggested by ^{1}H-NMR spectra over titration experiments, which could not be fitted to a suitable binding model, probably because of a two-stages binding process), titration experiments were repeated in DMSO-d_6/20%H_2O (v/v). In this more polar and competitive mixture, both **43** and **44** retained a high binding affinity for SO_4^{2-} (K_{ass}: $>10^4$ M^{-1}, demonstrating the negligible effect of the different chirality of the two receptors), with the formation of the 1 : 1 adduct, and high selectivity over AcO^- [K_{ass}: 44.9 (**43**), 72.6 M^{-1} (**44**)] and BzO^- [K_{ass}: 17.1 (**43**), 29.7 M^{-1} (**44**)], the only anions that express detectable interactions with the two receptors in the same solvent mixture. Of note, the binding affinity for SO_4^{2-} of **43** and **44** resulted significantly higher than those observed for the analogous systems featuring thiourea groups instead of squaramide moieties (K_{ass}: 1282 and 775 M^{-1}), for the modified amino acid **45** (K_{ass}: 1116 M^{-1}) (Fig. 16), and related amino acid-based squaramides.[44] Moreover, Joliffe and co-workers observed that receptor structural analogues of **43** and **44**, but featuring shorter peptide side chain lengths, increased length and flexibility of the peptide backbone, and the increased number of electron withdrawing or hydrophilic groups present on the squaramide phenyl substituents did not alter significantly the binding affinity and selectivity towards SO_4^{2-} in DMSO-d_6/20%H_2O (v/v).[45]

To obtain insight into the possible binding mode of this class of receptors, the structure of the 1 : 1 $[\mathbf{43}(SO_4)]^{2-}$ adduct was modelled.[43] The results of calculations show the SO_4^{2-} anion wrapped by the receptor and forming seven H-bonds, of which four with the squaramide NH protons, two with the NH amide protons from the peptide backbone, and one with the carboxamide group (Fig. 16), in agreement with changes in the ^{1}H-NMR spectra upon titration with SO_4^{2-}.

Recently, the bis[squaramido]ferrocene receptor **46** has been reported for SO_4^{2-} binding and electrochemical recognition (Fig. 17).[46]

^{1}H-NMR binding studies were performed initially in DMSO-d_6 containing 1% of water by titrations of **46** with various anions as TBA salts. No changes in the ^{1}H-NMR spectrum of **46** were observed upon addition of Cl^-, HSO_4^-, and NO_3^-, while the more basic F^- and AcO^- caused NH deprotonation. SO_4^{2-} and $H_2PO_4^-$ strongly interact with **46** with formation of 1 : 1 adducts (K_{ass}: $>10^4$ M^{-1}) (in contrast to the 1 : 1 adduct with $H_2PO_4^-$, the 1 : 1 adduct with SO_4^{2-} resulted quite stable even in the presence of a large excess this anion). On passing to a more competitive aqueous medium (DMSO containing 20% of H_2O), it was possible by UV-Vis spectroscopy to quantify the K_{ass} values for the 1 : 1 adducts of **46** with SO_4^{2-} and $H_2PO_4^-$ (K_{ass}: 3.1×10^5 and 1.4×10^4 M^{-1}, respectively), which suggest a marked selectivity of the receptor for the former. Interestingly, the structural analogue of **46** featuring only one squaramide moiety linked to the ferrocene unit shows in DMSO-d_6 containing 1% of H_2O a much lower selectivity for SO_4^{2-} with respect $H_2PO_4^-$, and an association constant (measured by ^{1}H-NMR titrations) for the formation of the 1 : 1 adduct with SO_4^{2-} (K_{ass}: 1.2×10^3 M^{-1}) that is over two orders of magnitude lower than that measured for **46** in DMSO containing 20% of H_2O, thus suggesting a higher efficiency of the scaffold having two stacked squaramide units in **46** for SO_4^{2-} binding.

Chloride binding is of high interest due to the fact that the transport of this anion through channels is particularly relevant from a biological point of view (see the Anion transport section). Muthyala and co-workers have demonstrated that the insertion of carbonyl groups such as benzoyl groups on the squaramide skeleton facilitates chloride binding in polar solvents such as CH_3CN by disrupting the intermolecular H-bonds between the carbonyl group of the substituents and the squaramide NHs which is instead favoured in apolar solvents such as $CHCl_3$.[47] The same authors have lately shown that these types of receptors can be used to detect chloride *via* excited state intramolecular proton transfer (see the Anion sensing section).

The tripodal receptor **47** (Fig. 17) was successfully employed for the development of ion selective electrodes (ISEs) to selectively sense chloride in sweat and blood samples.[48] Interestingly, the membranes prepared incorporating **47** were found to have a high selectivity towards chloride over commonly found interferents such as salycilate (often found in patients treated with aspirin) and heparine (used as the anti-coagulant).

Squaramide derivatives can be successfully employed for the development of interlocked structures such as rotaxanes[49] which were used, for example, for sodium halide ion pair recognition.[50] Very recently, Evans and co-workers have found that the addition of chloride to a solution of chiral 2-rotaxane **48** in $CDCl_3$ caused the shuttling of the macrocycle from the squaramide station to the diphenyl stopper (Fig. 18) as demonstrated by ^{1}H-NMR experiments with a measured association constant K_{ass} of 1300 M^{-1}.[51]

Anion extraction

Recently, it has been discovered that squaramides can be used to develop efficient methods to extract cations, anions, and ion-pairs.

Romański and coworkers have been very active in the field. They have developed various squaramide-based receptors (Fig. 19) that have been successfully used as extractants.[52–60]

As shown in Fig. 19, all the receptors developed in Romański's lab are characterised by the presence of at least one squaramide unit and one crown-ether unit, which are responsible for the binding of anions and cations, respectively. Indeed, receptors **49–57** are able to extract ion-pairs from water solution. As an example, receptor **50**, presenting a squaramide unit non-symmetrically substituted with a 3,5-trifluoromethylphenyl moiety and a benzo-18-crown-6 unit, acts as an efficient extractant for potassium sulphate in liquid/liquid extraction (LLE) technology. It is well known that benzo-18-crown-6 is highly specific for potassium cation binding and this also improves the anion affinity (K_{ass} = 2300 and 4300 M^{-1} for NaCl and KCl, respectively in CH_3CN/5% H_2O for the formation of the 1 : 1 complex, calculated from UV-Vis titrations). Interestingly, receptor **50** formed the 1 : 1 adducts with Cl^-, I^-, NO_2^-

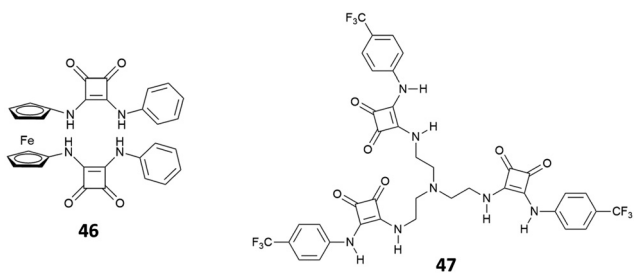

Fig. 17 Molecular structures of bis[squaramido]ferrocene **46** and tripodal receptor **47**.

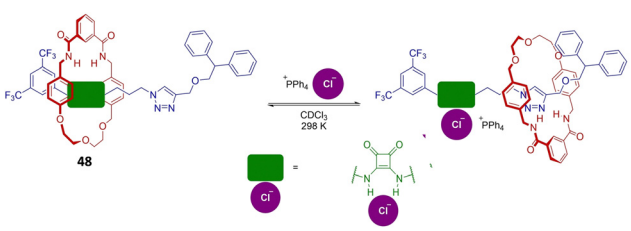

Fig. 18 Scheme of the shuttling of the macrocycle in rotaxane **48** induced by the addition of chloride in $CDCl_3$. Adapted with permission from ref. 51. Copyright Wiley 2023.

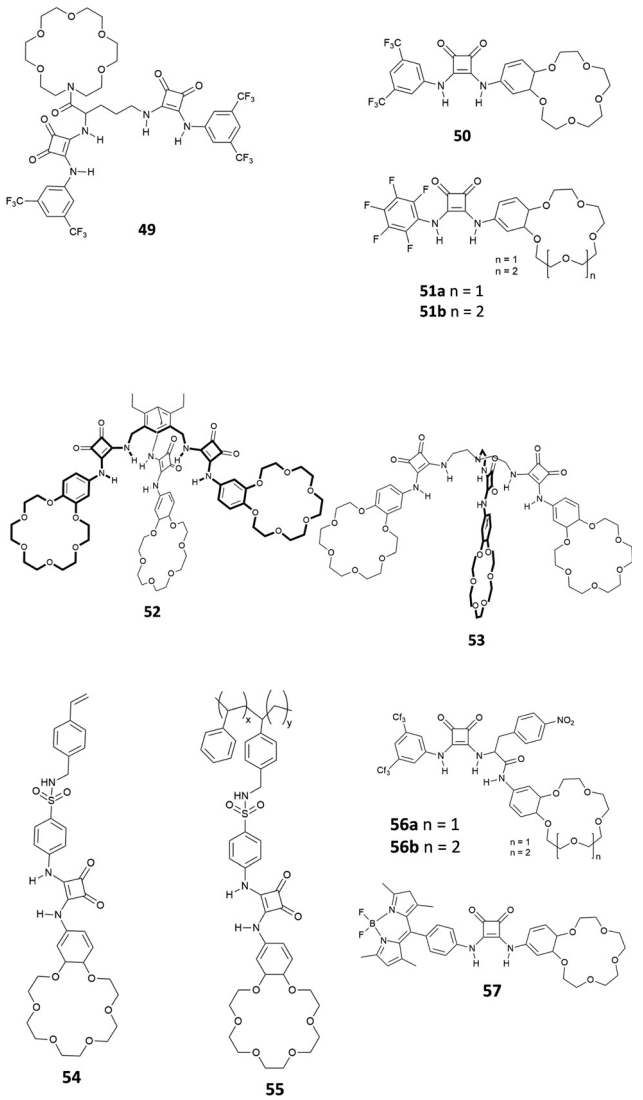

Fig. 19 Receptors **49–57** developed by Romański and co-workers for ion-pair extraction.

and NO_3^-, while in the case of SO_4^{2-} a peculiar supramolecular assembly formed by the 4:1 receptor/anion adduct was observed. The formation of the self-assembled structure was demonstrated by ^{1}H-NMR titrations in CD_3CN and DOSY-NMR (a decrease of 28% of the diffusion coefficient of the free receptor was measured), dynamic light scattering (DLS) experiments (an hydrodynamic diameter, d_H, of 28 nm for the supramolecular assembly was measured) and single crystal X-ray diffraction analysis on the crystals obtained by slow diffusion of diethyl ether vapours into a methanol solution of receptor **50** in the presence of an excess of Na_2SO_4 (Fig. 20). The authors demonstrated for the first time the possibility to extract a highly hydrophilic anion such as SO_4^{2-} from an aqueous solution of an alkaline earth salt to an organic phase. A ^{1}H-NMR experiment was carried out by adding a 2 mM solution of **50** in $CDCl_3$ aqueous solutions 50 mM of various anions (Cl^-, Br^-, NO_3^-, NO_2^-, $H_2PO_4^-$, and SO_4^{2-}) as their potassium salts. To confirm the importance of the counter

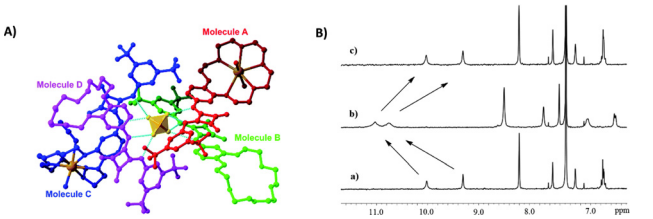

Fig. 20 Crystal structure of the supramolecular assembly formed by Na_2SO_4 and receptor **50** (A). Changes in the chemical shift of selected protons of receptor **50** in $CDCl_3$ before (a) and after (b) the addition of an aqueous solution of K_2SO_4 (B). The spectrum (c) is referred to a back extraction experiment and shows the reversibility of the process. Reproduced with permission from ref. 52. Copyright RSC 2019.

cation, Na_2SO_4 was also tested. In all cases, except for K_2SO_4, the formation of insoluble solids was observed confirming the unique properties of receptor **50** to increase the solubility of the SO_4^{2-} salt in organic solvents. Indeed, as shown in Fig. 20(B), a dramatic shift of the squaramide NH signals was observed when a solution of **50** was in contact with the aqueous solution of K_2SO_4. Back extraction experiments showed the ability of **50** to release the salt back to water.

Jolliffe and co-workers have also shown that squaramides can promote SO_4^{2-} extraction. In this case, the macrocyclic receptor **58** was employed.[40] LLE experiments were conducted by vigorously shaking a water solution containing TBA_2SO_4 with a $CDCl_3$ solution containing receptor **58** and analysing the organic phase by ^{1}H-NMR spectroscopy and it was demonstrated that one equivalent and even a substoichiometric concentration of SO_4^{2-} could be extracted from the aqueous phase. However, in contrast to what was observed by Romański, the lipophilicity of the counter cation was crucial in this case as Na_2SO_4 could not be extracted. In a competitive experiment, it was found that a $CDCl_3$ solution of receptor **58** could selectively extract SO_4^{2-} from an aqueous solution containing both SO_4^{2-} and NO_3^- and that a full recovery of SO_4^{2-} could be obtained by precipitating it back in water in the form $BaSO_4$ by using aqueous $Ba(NO_3)_2$ and forming the adduct **58**·NO_3^- *via* an anion metathesis process. Starting from these results, a U-tube experiment was designed (Fig. 21) and the sulfate transport across a bulk chloroform membrane was demonstrated in a wide pH range (pH = 3.2–9.4). In this experiment, the SO_4^{2-} extraction from the organic phase was monitored *via* ICP-MS using $BaSO_4$ gravimetric analysis. SO_4^{2-} transport was possible only in the presence of NO_3^- in the organic phase while a 2-fold increase in the transport rate was observed in the presence of $BaCl_2$ in solution, which drove the equilibrium by the Le Chatelier principle.

Interestingly, Maniesotis, Baggiani and co-workers showed that polymerisable squaramides **59** and **60** (already employed to prepare imprinting polymers)[61] could be used for producing molecularly imprinted polymers (MIPs) for the solid state extraction of 4-hydroxy-3-nitrophenylarsonic acid (commonly known as roxarsone), an organoarsenic compound used in poultry production as a feed additive (Fig. 22).[62] Monomers **59** and **60** showed good association constants for the formation

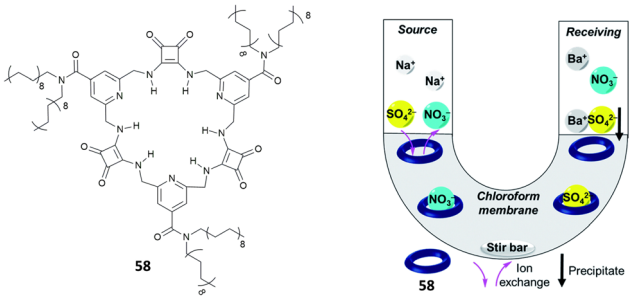

Fig. 21 Structure of receptor **58** and scheme of the U-tube test to demonstrate sulfate transport across the chloroform membrane. Reproduced with permission from ref. 40. Copyright RSC 2020.

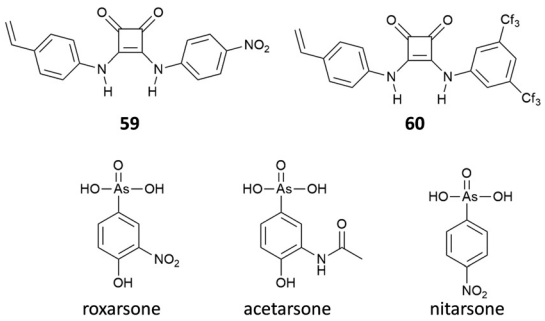

Fig. 22 Squaramides **59** and **60** used to prepare MIPs for the solid-state extraction of the organoarsenic compound roxarsone. The structures of roxarsone analogues acetarsone and nitarsone are also reported.

of 2 : 1 adducts with roxarsone as its TBA salt in the range of 10^3 M^{-1} in DMSO-d_6 measured by ^{1}H-NMR titrations. Imprinting polymers were prepared by mixing monomers and roxarsone salt in a 2 : 1 ratio with the cross-linker dimethylacrylate (EDMA) and the free-radical initiator 2,2′-azobis(2,4-dimethyl)valeronitrile (ABDV). Imprinting polymers showed similar affinity towards roxarsone than the monomers but in the more competitive solvent methanol (K_{ass} = 14.65 × 10^3 M^{-1} and 16.85 × 10^3 M^{-1}, for the MIP prepared with **59** and **60**, respectively). In terms of selectivity, a remarkable selectivity towards roxarsone when compared to its analogous acetarsone and nitarsone was observed for MIP based on squaramide **60**.

This MIP was successfully used to establish a protocol for the solid state extraction of roxarsone by loading polypropylene solid-phase extraction cartridges with the MIP and then putting it in contact with an aqueous sample containing the target analyte. Cartridges were then washed, and the eluates were analysed by HPLC. With this method, it was possible to measure concentrations of roxarsone down to 1 μg mL^{-1} in water samples.

Very recently, Jolliffe and co-workers have shown a novel strategy for developing squaramide copolymers by combining together poly(ethylene glycol) methyl ether methacrylate (PEGMA) and [(*tert*-butoxycarbonyl)amino]ethyl methacrylamide (Boc-AEMA) in different ratios and functionalising the resulting polymer with squaramides bearing various substituents (3,5-(bis)-trifluoromethylphenyl and 2-fluornyl) after the removal of the Boc group. The polymers showed the ability to

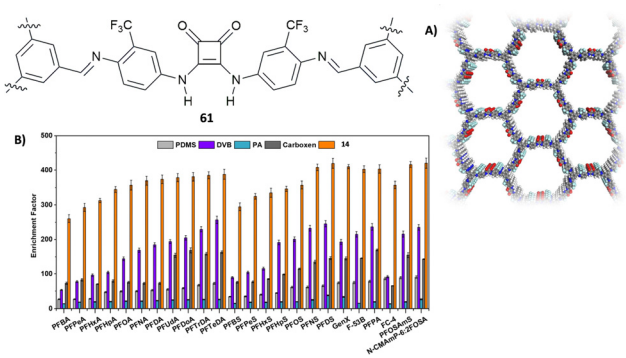

Fig. 23 Structure of squaramide-based COF **61** and its structure obtained by PXRD (A). Enrichment factor for a family of PFAS for COF **61** and other commercially available extractants (B). Reproduced with permission from ref. 64. Copyright Wiley 2022.

bind anions in DMSO with no selectivity and similarly to the corresponding molecular squaramides while no binding was observed in pure water.[63]

A fluorinated squaramide-based covalent organic framework (COF) (**61**, Fig. 23(A)) that is able to efficiently extract a broad-spectrum of per- and polyfluoroalkyl contaminants from water was described by Zheng, Ouyang and co-workers.[64] COF **61** allows for multiple interactions with PFAS as it is able to act as the H-bond donor and H-bond acceptor and has fluorophilic moieties. The PFAS chosen for the extraction measurements comprise, among others, PFOA (perfluorooctanoic acid, in its anionic form), PFOS (perfluorooctane sulfonate), GenX (2,3,3,3-tetrafluoro-2-(1,1,2,2,3,3,3-heptafluoropropoxy)propanoic acid, in its anionic form), F-53B (chlorinated polyfluorinated ether sulfonate), the cationic PFOSAmS (perfluorooctaneamido quaternary ammonium salt), and the zwitterionic *N*-CMAmP-6:2FOSA (*N*-(carboxymethyl)-*N*,*N*-dimethyl-3- (((3,3,4,4,5,5,6,6,7,7,8,8,8-tridecafluorooctyl)sulfonyl)amino)1-propanaminium). Glass capillaries etched with HF were covered with COF **61** by dip-coating technology and immersed into a water solution spiked with PFAS. The extraction performance was analysed by measuring the areas of the mass spectra of the pollutants. As shown in Fig. 23(B), COF **61** showed a higher enrichment factor (that measures the overall success of the extraction) than other commonly used commercially available extractants such as PDMS (polydimethylsilossane), DVB (divnylbenzene), PA (polyacrylate), and carboxen.

Anion sensing

Since their introduction as receptors for the molecular recognition of anions,[15] squaramide-based systems for anion binding and sensing represented an active field of research. Similarly, to the case of imidazole-, pyrrole-, urea- or amide-based systems, the design of squaramide-based molecular sensors has undergone significant developments, involving different approaches. Among these, one of the simplest involves the use of host–guest complexes between a receptor and a specific indicator, to be used in the so-called indicator displacement assays (IDAs).[65]

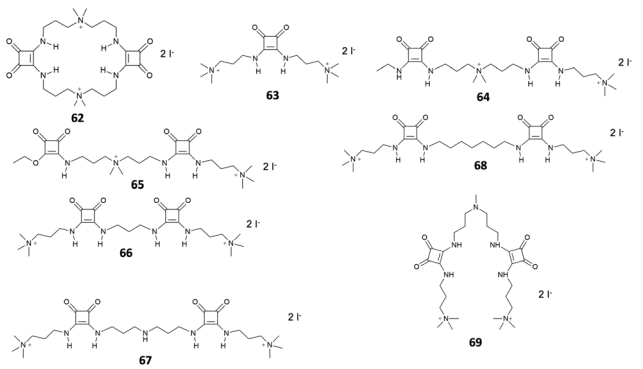

Fig. 24 Receptors **62–69** developed by Costa and co-workers.

This strategy exploits the competition between the indicator and the target analyte in interacting with the receptor, producing a detectable response, such as changes in color or fluorescence emission, when the indicator is displaced from the receptor. Examples of this approach in squaramide-based systems were described in an early work by Costa *et al.*, which focused on different families of squaramide-ammonium charge-assisted receptors (Fig. 24). Their design allows the combination of electrostatic interactions and hydrogen bonds to target oxyanions, such as sulfate and hydrogen phosphate, in aqueous media.[66–68]

The anion binding ability of receptor **62** towards different anions was investigated by NMR and isothermal titration calorimetry (ITC).[68] The results show a reduced binding ability of receptor **62** towards nitrates, halides and other monoanions, due to the selectivity promoted by the two tetra-alkylammonium groups. The authors suggested that the selectivity towards sulfates over other divalent anions might be due to constrains imposed by the squaramide functions, which favors interactions with tetrahedral sulfate anions. In the presence of fluorescein disodium salt, receptor **62** produced a quench of the fluorescein emission, as the consequence of a photo-induced electron transfer (PET) process from the squaramide donor to the excited singlet state of the fluorophore. Upon addition of sulfate anions, the PET is suppressed due to the complexation of the competing anion, restoring the fluorescence emission of the non-complexed fluorescein.

Receptors **63–68** were designed to work in a similar fashion.[66] Different from receptor **62**, this family was based on a linear molecular skeleton, showing subtle differences in the H-bonding capability and in the spacing between the charged sites, with distances between the electropositive sites that increase from receptor **63** to receptor **68**. In this case, the sensing was achieved using a colorimetric ensemble, exploiting the acid–base equilibrium of the common pH indicator cresol red. When complexed by receptors **63–68**, the indicator showed a purple coloration. This corresponds to the dianionic semiquinone form, which is preferentially complexed by receptors **63–68**. The color turned to yellow upon addition of dianions such as HPO_4^{2-} and SO_4^{2-}. The selectivity of the ensembles was also investigated in the presence of potential competitive anions such as F^-, Cl^-, Br^-, I^-, CO_3^{2-} and NO_3^- in EtOH/H_2O mixtures (9 : 1 v/v). The results showed a slight affinity towards sulfate over phosphates. This was particularly evident for receptor **68**, which showed a relative sulfate/phosphate selectivity ratio of 2.28.

The choice of the indicator can also affect the selectivity of the IDA towards specific anionic species. In a more recent article, Costa *et al.* described two IDAs based on receptor **69** complexed with cresol red and bromocresol green, respectively.[67] In the presence of different anionic species in mixtures of EtOH/H_2O (9 : 1, v/v), both IDAs produced a positive response only in the presence of phosphate and sulfate. In particular, phosphate and sulfate both produced a positive IDA response with cresol red, while bromocresol green proved to be selective only for the sulfate anion. On the basis of these results, the author implemented this approach using a UV-Vis microplate reader, enabling the parallel quantitative detection of these two anions by comparison with calibration curves.

In a further development of this approach, Costa, Alarcon, Garcia-Espana *et al.*[69] designed a squaramide based boehmite-(**70**) or silica-coated boehmite (**71**) IDAs, decorated with charged alkylammonium groups, able to complex bromocresol green (Fig. 25). The system works in a similar fashion as described above; however, different to the previous systems, this has the advantage to produce, among different anions, a selective response toward carboxylates and sulfates in pure water. The authors pointed that none of the previous systems were able to produce such a selective response in pure water and attributed this behavior to the presence of the nanoparticle substrate.

Morey *et al.*[70] developed magnetic squaramide-coated Fe_3O_4 nanoparticles **72** for the detection of carboxylates, based on receptor **73** (Fig. 26). In this case, the nanoparticles were pretreated with a buffered (pH = 8) solution of fluorescein (2×10^{-5} M). This system was then tested with solutions of different anionic species (mono, di, tricarboxylates, F^-, Cl^-, Br^-, NO_3^-, PO_4^{3-} and SO_4^{2-}), also in competing media such as water. The displacement of the fluorescein and the consequent increase of the emission at 490 nm was observed only in the case of mono and dicarboxylates. As pointed out by the authors,

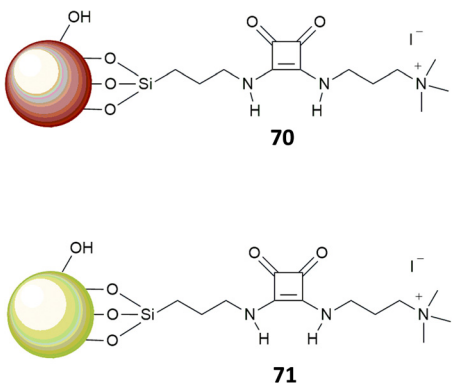

Fig. 25 Receptors **70–71**.

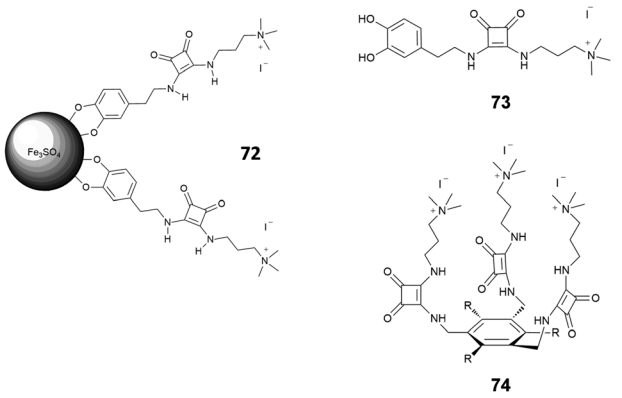

Fig. 26 Receptors **72–74**.

this system shows a selectivity analogous to that of more pre-organized receptors such as **74**, previously published.[71]

A typical approach to the design of chemosensors, consists of a receptor covalently linked to a signaling unit, either directly or *via* a spacer. The interaction between the receptor unit and the analyte produces a specific response that depends, in the first place, to the intrinsic properties of the signaling unit. Accordingly, depending on the type of signaling unit, a chemosensor can be defined as fluorescent, colorimetric or redox. This strategy has been largely applied for designing chemosensors for different analyte sensing, including anions. Recently, it has also been applied to squaramide based systems.

Jolliffe *et al.*[72] described four chemosensors for anions (**75–78**), consisting of aryl substituted squaramides covalently bonded to a luminescent anthracene moiety (Fig. 27). The choice of different electron-withdrawing aryl substituents and different positions of substitution (3,5-CF_3, 4-CF_3, 4-NO_2) allowed a modulation of the acidity/H-bonding ability of the squaramides. The sensing ability of the four receptors was investigated upon addition of different halides (F^-, Cl^-, I^-, and Br^-) and NO_3^- anions. The systems showed a selective response only upon the addition of Cl^- anions, producing a quenching of the fluorescence. Specifically, receptors **75–77** exhibited a quench of the excimer emission at 530 nm, which was less evident on passing from **75** to **77**, suggesting an influence of the substituents (*i.e.*, type, position and number of substituents) in modulating the optical response.[73,74] No particular changes in the fluorescence emission were observed for the less acidic receptor **78**.

The response is attributed to the formation of a 1 : 1 complex *via* H-bonding, as suggested by ^{1}H-NMR and a solid-state analysis by single crystal X-ray diffraction. However, in the presence of a large excess of Cl^-, receptors **75–77** showed an unusual example of deprotonation of a receptor by Cl^-, as suggested by the disappearance of the ^{1}H-NMR signals observed for the NH protons at high concentrations of this anion. The deprotonation was also evidenced by dramatic naked-eye color changes observed for **75–77**, making these systems suitable also for colorimetric detection of Cl^- anions *via* deprotonation of the squaramide NHs. Deprotonation induced by anions represents in fact another strategy for anion sensing and exploits the development of acidic receptors able to produce a change in color upon partial or complete deprotonation of the H-bond donor sites.[75] This approach has been applied to several urea-based systems,[76,77] and squaramide-based receptors have also been the subject of a number of recent studies.[78–80] The first example of squaramide-based colorimetric receptors for anions (Fig. 28) has been developed by the Taylor group,[81] which investigated the sensing ability of electron-deficient receptors **79–81** towards different anions and compared their behavior with that of *N*,*N*-bis(dinitrophenyl)urea (**82**).

In a very recent work, Lane and Jolliffe[82] described a case of colorimetric sensors as a part of a more general study, aimed at investigating the influence of the direct receptor–fluorophore conjugation in anion sensing. The authors compared the sensing ability of a family of squaramide-based chemosensors (**83–90**) functionalized with different fluorophores (Fig. 29), *via* both, a direct conjugation or a methylene spacer. The results suggest that direct conjugation has a strong effect in increasing the acidity of the NHs, probably due to the higher stabilization by electronic delocalization of the deprotonated species. This is reflected in the response of the conjugated receptors in the presence of anions. In particular, receptors **84–86** undergo deprotonation upon addition of 50 equiv. of different anions, accompanied by a color change, according to the basicity of the anions (yellow in the absence of anions, orange for the mono-deprotonated receptor and deep blue for complete deprotonation). Receptor **83** showed a different behavior. An investigation

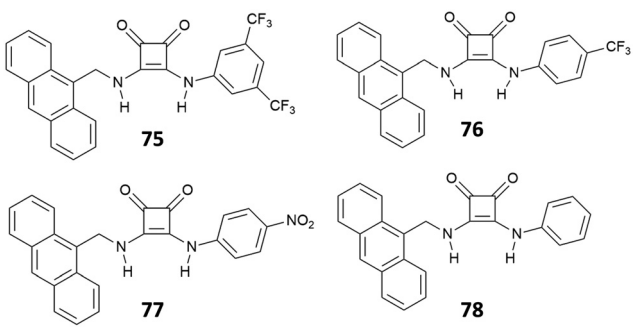

Fig. 27 Receptors **75–78**.

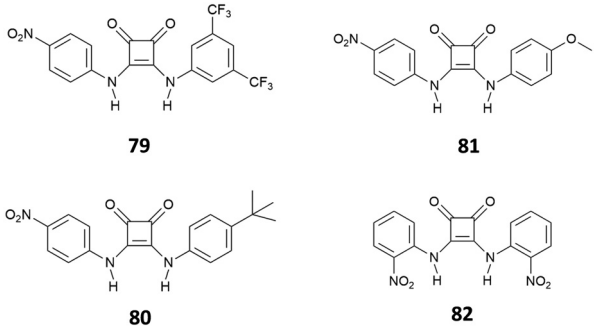

Fig. 28 Receptors **79–82**.

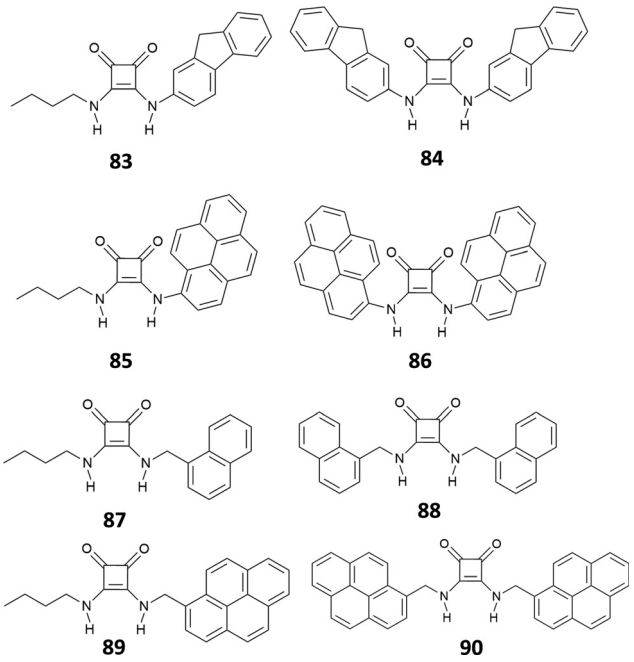

Fig. 29 Receptors **83–90**.

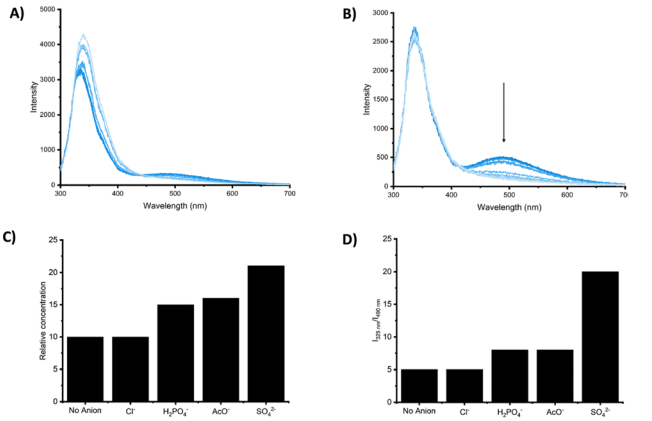

Fig. 30 Emission spectra of **87** (20 μM) in DMSO (1% H_2O) upon addition of TBA_2SO_4 (0 to 60 equiv.) (λ_{ex} = 280 nm) at 298 K (A). Emission spectra **88** (20 μM) in DMSO/1%H_2O upon addition of TBA_2SO_4 (0 to 80 equiv.) (λ_{ex} = 280 nm) at 298 K (B). The ratios of I_{325}/I_{490} for **87** (C) and **88** (D) in DMSO/1%H_2O at 298 K in the presence of anion (10 equiv.). Adapted with permission from ref. 82. Copyright RSC 2023.

by UV-Vis spectroscopy showed a red shift in the maximum absorbance only in the presence of monovalent oxyanions, mainly $H_2PO_4^-$, AcO^-, consistent with a 1 : 1 binding model. Although this response was even more pronounced in the presence of SO_4^{2-}, it was not possible identifying the binding model, probably due to complex equilibria involved. Receptors bearing a methylene spacer, **87–90**, showed neither deprotonation nor changes in the UV-Vis spectra upon addition of anionic species. This was attributed to the methylene spacer that insulate the squaramide receptor from the substituents.

While the fluorescence response of **83–86** in the presence of anions could not be investigated, due to the deprotonation or the shift of the absorbance maximum, **87–90** showed an interesting behavior. The emission spectra of **87** and **88** showed two bands at 325 nm and 495 nm, attributed to the monomer and the excimer, respectively. Dilution experiments suggested that the excimer is the result of intermolecular aggregation rather than intramolecular interactions promoted by a *syn–syn* conformation of the receptor. Upon addition of $H_2PO_4^-$, AcO^- and SO_4^{2-}, **87** and **88** responded with a decrease of the emission intensity of the excimer band, with a more pronounced effect observed for **88** and, in general, a greater response in the presence of SO_4^{2-} (Fig. 30).

Receptor **86** was also the object of a recent study by Caltagirone *et al.*[83] The anion binding ability of the receptor towards a number of anions (F^-, Cl^-, Br^-, I^-, CN^-, and BzO^-) was investigated by ^{1}H-NMR, UV-Vis and fluorescence spectroscopy in DMSO (DMSO-d_6)/0.5%H_2O. The results showed deprotonation in the presence of BzO^-, CN^- and F^-, accompanied by a chromatic change of the solution, from colorless to yellow. Among the remaining halogenides, **86** showed a low affinity only upon addition of Cl^-. This was explained considering that DMSO represents a competing molecule for the interaction with the squaramide, as suggested by the tendency of this receptor to form solvate phases in the solid state. In less competing solvents, such as CH_3CN, **86** showed a higher affinity for Cl^- anions. Investigation of the fluorescence response toward different anions suggested a scarce ability of **86** to operate as fluorescence molecular sensors for anion species. This was attributed to the steric hindrance in the receptor molecule, probably due to the direct conjugation between the pyrene moiety and the squaramide core. Previous studies[84] suggest that increasing the flexibility of the system by adding an alkyl spacer might improve the response.

In this case, this was achieved using an alternative approach. Indeed, in the presence of copper(II) ions, **86** formed a 2 : 1 metal-to-ligand complex, accompanied by a naked eye detectable fluorescence emission (Fig. 31). Among different cations, **86** selectively responded to copper(II), producing an emission band at 480 nm (λ_{exc} = 350 nm). Upon addition of anions, the 2 : 1 metal-to-ligand complex showed a variation of the fluorescence emission only in the presence of excesses of basic anions, resulting in a naked eye detectable change from green to a pale red (under a UV lamp). This was attributed to the deprotonation of the squaramide NHs of the metal complex, which caused the formation of a red-shifted emission band. The authors speculated that the 2 : 1 metal complex could be used as a fluorescence chemodosimeter to recognize basic anions.

The same authors recently described a family of macrocyclic and non-cyclic bisquaramide receptors (**16–17** and **19–20** respectively), directly conjugated to a dansyl moiety.[19] These receptors have been investigated as potential fluorescent probes for the recognition of salted forms of naproxene and chetoprofen (see the Anion binding section).

Another example of macrocyclic receptors was reported by Romański *et al.*,[85] which developed a family comprising a

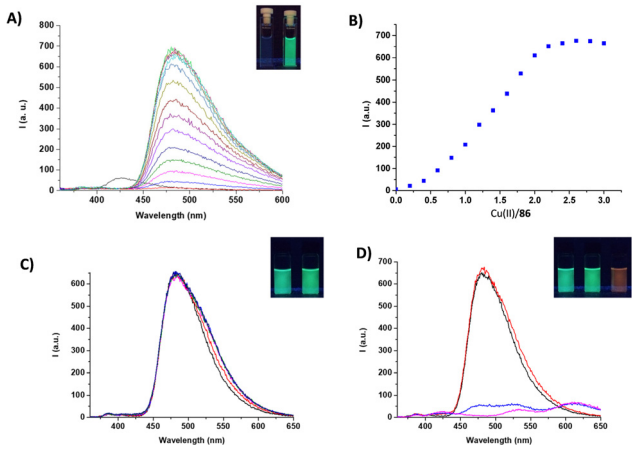

Fig. 31 Emission spectra of **86** (1.0×10^{-5} M) in CH_3CN upon addition of $Cu(ClO_4)_2$ hydrate (2.5×10^{-3} M), λ_{exc} = 350 nm (A) (inset: naked-eye colour change of **86** in the presence of 2 equiv. of $Cu(ClO_4)_2$ hydrate). The plot reporting the fluorescence emission intensity (480 nm) *versus* molar ratio relative to the titration of **86** with $Cu(ClO_4)_2$ hydrate (B). The emission spectra of the **86**–Cu(II) complex (2.5×10^{-5} M) in the presence of increasing amounts of TBACl (2.5×10^{-3} M, λ_{exc} = 350 nm) (C) (inset: naked eye emission of **86** and upon addition of 10 equiv. TBACl). The emission spectra of the **86**–Cu(II) complex (2.5×10^{-5} M) in the presence of increasing amounts of TBAOH (2.5×10^{-3} M, λ_{exc} = 350 nm) (D) (inset: naked eye emission of **86**–Cu(II) complex, upon addition of 2 equiv. and 6 equiv. of TBAOH). Adapted with permission from ref. 83. Copyright MDPI 2021.

simple squaramide based macrocyclic receptor for anions (**91**) and its ditopic analogues linked respectively to one (**92–93**) or two (**94**) benzo-18-crown-6 moieties (Fig. 32). In addition, in the case of **93**, a fluorescent naphthalene moiety was also incorporated into the macrocyclic receptor, providing a platform suitable for ion pair sensing. The anion and ion pair ability of **91** and **92** were investigated by ^{1}H-NMR, also comparing the influence of the cations in enhancing the binding ability.

The results suggest that, in general, anion binding occurs preferentially *via* hydrogen bonds involving the squaramide NHs rather than the amide donors. Among the anions tested, these receptors showed a higher affinity towards V-shaped and tetrahedral anions, such as benzoate and sulfates. In general, the ditopic receptors, due to the presence of the electron donating alkoxy groups, showed a weaker anion recognition

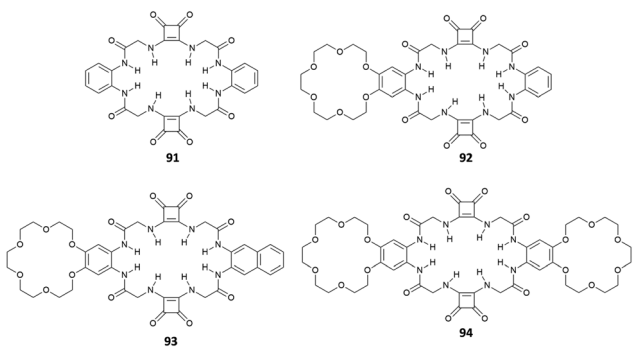

Fig. 32 Structures of receptors **91–94**.

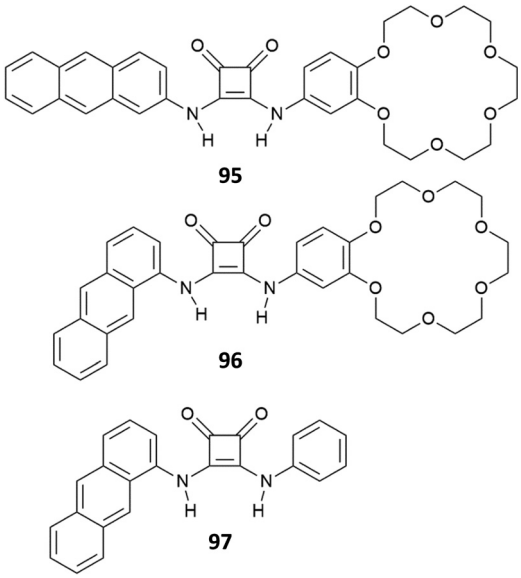

Fig. 33 Structures of receptors **95–97**.

with respect to monotopic **92**; however, in the presence of cations such as Na^+ and K^+, an enhanced binding is observed. The optical response of **93** towards different anions was also characterized. **93** produced a selective optical response in the presence of sulfate anions which consists of a bathochromic shift from 291 nm to 296 nm in the electronic absorption spectrum. Furthermore, the emission spectra showed an increase of the fluorescence emission and a concomitant formation of a new band at 420 nm. **93** was also tested as an optical ion pair sensor, responding in the presence of potassium sulfate.

In a second article, Romański *et al.*[86] described a family of luminescent squaramide-based receptors analogous to that reported by Elmes *et al.*[72] Receptors **95–97** (Fig. 33) show an anthracene moiety as a fluorogenic unit. Furthermore, **95** and **96** bear a macrocyclic unit capable of complexing metal ions, making these systems suitable for ion pair detection (see the Anion extraction section). The presence of the metal ion in the macrocyclic cavity induced an enhancement of the affinity towards anions. Receptor **95** selectively extracts SO_4^{2-} salts from aqueous and organic phases, providing quenching or an increase of the fluorescence, depending on the water content in the receptor solution.

A family of redox chemosensors (**98–100**) was recently developed by the same authors,[87] using the same molecular skeleton proposed for **95** and **97**, only differing for the replacement of the fluorescent anthracene moiety with a ferrocene redox signaling unit (Fig. 34). The family consists of a monotopic receptor **100**, and two ditopic receptors **98** and **99**, obtained by linking the squaramide receptor to 15-crown-5 ether and an 18-crown-6 ether, respectively. The binding ability of these systems towards cations and ion pairs was characterized *via* different techniques, including single crystal X-ray diffraction, spectrophotometric, spectroscopic, and electrochemical measurements. The choice of different cavity sizes was reflected in different

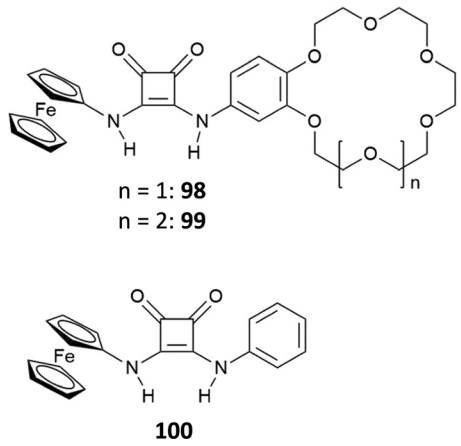

Fig. 34 Structures of receptors **98–100**.

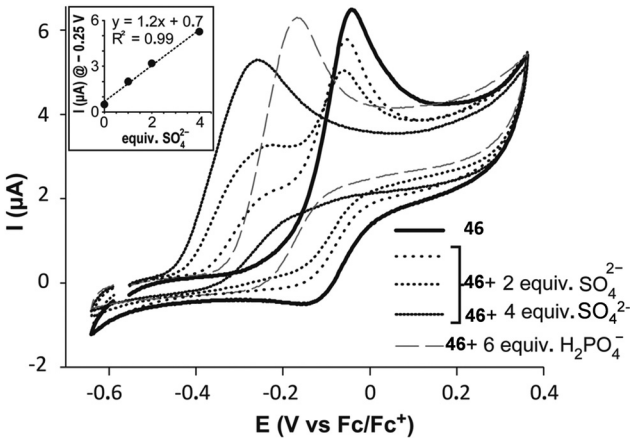

Fig. 35 Cyclic voltammetry of **46** (0.25×10^{-3} M) in DMSO/20%H_2O, after addition of 2, 4 equiv. of $(TBA)_2SO_4$ and 6 equiv. of $TBAH_2PO_4$ (0.1 M $TBAClO_4$) at a scan rate of 100 mV s^{-1} and T of 80 °C. Inset: electrochemical response of **46** after addition of SO_4^{2-} at −0.25 V *vs.* Fc/Fc^+. Reproduced with permission from ref. 46. Copyright RSC 2022.

selectivities towards cations. **98** moderately captured Na^+ ions (K_{sodium} = 9400 M^{-1}) while **99** showed strong binding with both Na^+ (K_{sodium} = 25 900 M^{-1}) and K^+ ($K_{potassium}$ = 144 200 M^{-1}), though showed higher selectivity towards K^+. The binding ability of **98–100** in the simultaneous presence of anions and cations showed a behavior consistent with that previously observed. Due to the absence of the electron donating alkoxy groups of the ditopic receptors **98** and **99**, the monotopic receptor **100** showed the strongest anion binding ability. However, in the presence of Na^+ or K^+ cations, acetonitrile solutions of **98** and **99** showed an enhanced binding. This effect was attributed to the presence of the cations in the macrocylic cavity, which increased the hydrogen bond donor nature of the squaramide function, influencing the strength of the interactions with the anionic species. The sensing ability of **98–100** towards different anions was investigated in the presence or absence of Na^+ or K^+ cations by cyclic voltammetry measurements. The results showed that, upon the addition of different anions, the presence of Na^+ or K^+ cations induced a more significant response in oxidation potentials when compared to that measured in their absence. In particular, for **98**, this effect was observed in the presence of Na^+, while, for **99**, with both Na^+ and K^+ cations.

A further example of redox sensors was recently reported by Jolliffe, Bowman-James and Adriaenssens[46] which reported the binding and sensing ability of the bis[squaramido]ferrocene **46** (for a description of the anion binding properties of receptor **46** see the Anion binding Section). Receptor **46** showed an irreversible oxidation at −63 mV *vs.* Fc/Fc^+ with the anodic current that was about 3 times higher than the cathodic one. Upon the addition of SO_4^{2-} or $H_2PO_4^-$, a two-wave behavior was observed (Fig. 35).

In particular, the new wave corresponding to the oxidation of the 1 : 1 adduct of **46** with the SO_4^{2-} anion resulted significantly shifted to more a negative potential ($\Delta E_{1/2}$ = 242 mV *vs.* free **46**) as compared to the wave recorded for the adduct with $H_2PO_4^-$ ($\Delta E_{1/2}$ = 107 mV *vs.* free **46**), in agreement with the higher affinity of **46** for SO_4^{2-} than that for $H_2PO_4^-$. Furthermore, for SO_4^{2-}, the anodic current increased linearly when the concentration of the anion was increased up to 4 equiv. (Fig. 35).

The recognition of guest species exploiting the variation of emission due to an excited-state intramolecular proton transfer (ESIPT) mechanism represents another approach for anion sensing. In an ESIPT process, a proton of the chromophore is transferred after photo-excitation from an HB-donor (generally amines or hydroxyl groups) to a nearby HB-acceptor (for example N, O and S) producing a fast enol–cheto phototautomerization.[65] Therefore, molecules featuring ESIPT require the presence of an intramolecular hydrogen bond within the chromophore to allow the proton transfer. In general, ESIPT can produce variable luminescence phenomena (for example dual emission), large Stoke shifts and is very sensitive to the surrounding environment. These features can be conveniently exploited for sensing and imaging.

Muthyala *et al.* proposed a sensing approach based on the suppression of ESIPT,[88] designing three squaramide-based receptors **101–103** (two *ortho*- and one *meta*-benzoyl squaramide derivatives) for the recognition of Cl^- anions (Fig. 36).

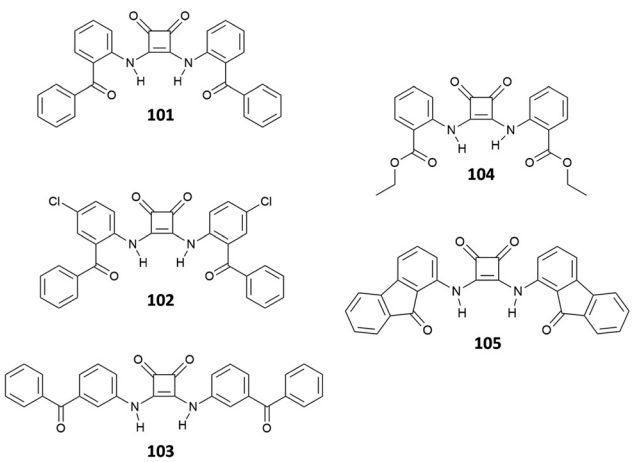

Fig. 36 Structures of receptors **101–105**.

The results highlighted differences in the behaviour between *ortho*- and *meta* derivatives. Specifically, the two *ortho*-derivatives showed a solvent polarity-dependent emission, not observed for the *meta*-derivative, with a decrease of fluorescence emission by a factor 1000, passing from acetonitrile to the lower polar chloroform. Furthermore, upon the addition of different halides in acetonitrile, *ortho*-squaramides produced an enhancement of the emission intensity only in the presence of Cl^- anions, while the *meta*-derivative showed a decrease of the emission irrespective of the anion added. The differences observed between *ortho*- and *meta*-substituted squaramides were ascribed to the ability of the formers to interact intramolecularly *via* hydrogen bonds between the N–H donors and the C=O acceptors. In the presence of polar solvents or anions, the intramolecular interaction was weakened or disrupted, suppressing the ESIPT and producing a variation of the fluorescence emission. In a more recent article, Muthyala *et al.*[89] investigated in more detail the emission enhancement promoted by Cl^- binding of *ortho*-substituted squaramides, investigating the three receptors **101** and **103–105** experimentally and computationally. The results suggest that this behaviour could ascribed to two degenerate excited states, resulting from two distinct competing charge transfer pathways. In the absence of anions, the emission is decreased due to the competition of these two pathways. The complexation of Cl^- suppresses one of the two charge-transfer pathways, resulting in the increase of the emission.

Due to their intrinsic features, such as the presence of strong hydrogen bond donors and the aromatic cyclobutenedione ring, squaramides tend to self-assemble *via* hydrogen bonds and π–π stacking. This ability has been exploited to design self-assembled systems able to respond to anion binding with changes in one of their properties, such as luminescence. There are different ways in which self-assembly or its perturbation can induce changes in the optical properties of the system. Examples of these are "aggregation-caused quenching" (ACQ), "aggregation-induced emission" (AIE) and "disaggregation-induced emission" (DIE).[90,91] In this respect, Elmes focused both on simple molecules[18,92] and more complex systems.[21]

In a recent work,[92] the two chemosensors **106** and **107** (Fig. 37(A)), consisting of a squaramide-based receptor linked *via* a short spacer to a naphtalimide fluorogenic unit, were investigated as chemosensors, exploiting a disaggregation-induced emission (DIE) mechanism to recognize halides. Self-assembly of **106** and **107** was investigated in solution and the solid-state. Investigation by ^{1}H-NMR at 298 K and 343 K showed a strong tendency to self-aggregate in aqueous solutions (Fig. 37(B)). Increasing the temperature resulted in disruption of the self-assembly of both **106** and **107**. Attempts to crystallize the two receptors from DMSO and obtain some insights into the self-assembly in the solid state resulted in the formation of amorphous materials, featuring interesting morphologies (Fig. 37(C)). Characterization of **106** and **107** by UV-vis and fluorescence spectroscopy showed three absorption bands at 280 nm, 340 nm, and 445 nm and an emission band at approximately 525 nm. In particular, by varying temperature in DMSO/5%H_2O, both **106** and **107** showed a dramatic

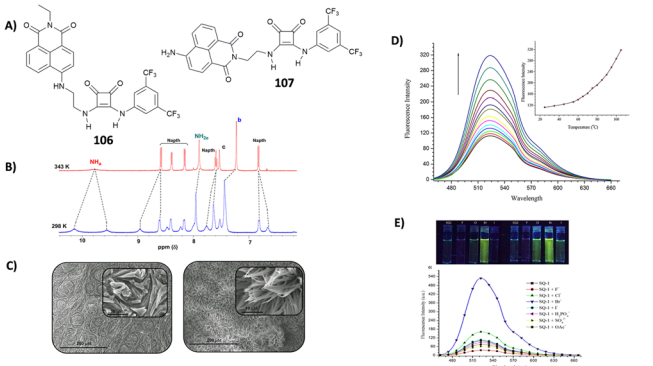

Fig. 37 Receptors **106** and **107** (A). ^{1}H-NMR spectra showing disaggregation phenomena when temperature is increased from 298 K (bottom) to 343 K (up) (B). Scanning electron microscopy (SEM) images of the solid-state self-assembly for **106** (left) and **107** (right) (C). Variable temperature fluorescence emission experiments (from 25° to 110 °C) in DMSO/5%H_2O, reported for **107** (5.0×10^{-6} M) (D). Fluorescence response of **106** (5 μM) in DMSO/5%H_2O upon addition of different anions (λ_{exc} 435 nm) (bottom), and fluorescence responses of **106** and **107** toward different halides in 5% aqueous DMSO as seen by the naked eye under a UV-vis lamp (top) (E). Adapted with permission from ref. 92. Copyright Frontiers 2019.

enhancement of the fluorescence emission (220–300%) as the temperature increased (Fig. 37(D)). This was attributed to the disaggregation promoted by the increase of temperature, as also suggested by the results of the ^{1}H-NMR variable temperature experiments (Fig. 37(B)). The anion binding ability of **106** and **107** was investigated in 0.5% aqueous DMSO-d_6 by ^{1}H-NMR, upon the addition of different anions (30 equiv.) as their TBA salts (AcO^-, $H_2PO_4^-$, SO_4^{2-}, Br^-, Cl^-, F^-, and I^-). Anions such as AcO^-, $H_2PO_4^-$, SO_4^{2-} and F^- showed a complex behavior, leading to disappearance or either sharpening or broadening of the NH signals. In particular, in the presence of F^-, both receptors underwent deprotonation, accompanied by a stark colour change of the solution, which turned from yellow to red. The other halides showed a significant downfield shift of the NH signals only in the presence of Cl^- and Br^-, suggesting interactions with these anions *via* hydrogen bonds. The results of the NMR titration fitted with a 1:1 binding model and produced association constants in the range of 100–500 M^{-1}. Based on these results, the authors investigated whether interactions with different anions promoted disaggregation, resulting in an enhancement of the fluorescence emission by DIE. Bases such as AcO^-, $H_2PO_4^-$, SO_4^{2-} and F^- promoted a quenching of the emission band at 525 nm. This, at least in the case of F^-, was attributed to the deprotonation. The addition Cl^- and Br^- anions induced a consistent enhancement of the fluorescence emission. In particular, Br^- produced the best response, resulting in an enhancement of the fluorescence emission of about 500% for **106** and 600% for **107** (Fig. 37(E)).

Anion transport

Since Costa and co-workers introduced the evidence that squaramide-based compounds were able to bind marvellously

both cations and anions, there has been an increasing interest in the exploiting their great anion binding properties, especially towards halogens such as chloride. On this basis, squaramide-based compounds represent excellent candidates as ionophores for the transmembrane transport of anion species such as chloride, bicarbonate, and sulphate.

The first example of squaramide-based ionophores for this purpose was reported by Gale and co-workers, one of the pioneers in the use of supramolecular architectures for transmembrane anion transport.[93] Squaramides **108–110** reported in Fig. 38, previously studied for their anion binding properties, were also tested for their capability to transport Cl^- across the synthetic membranes in comparison with their analogous urea- and thiourea-derivatives **A–F** (Fig. 39).

To investigate their transport activity, antiport Cl^-/NO_3^-, H^+/Cl^- or Na^+/Cl^- symport assays were conducted. The results reported in Fig. 40 demonstrate that squaramides **108** and **109** are able to transport Cl^- out of liposomes much faster than that of the analogous thioureas and ureas.

Nevertheless, similar results are obtained in the case of **110**. Indeed, the values of the EC_{50} obtained through the Hill analysis suggested that **108–110** are more efficient with respect to the analogous ureas and thioureas, in particular **109** and **110** (EC_{50} of **109** is about 4-fold and 7-fold higher than that of **C** and **D**, respectively, while EC_{50} of **110** is about 16-fold and 30-fold higher than that of **E** and **F**, respectively).

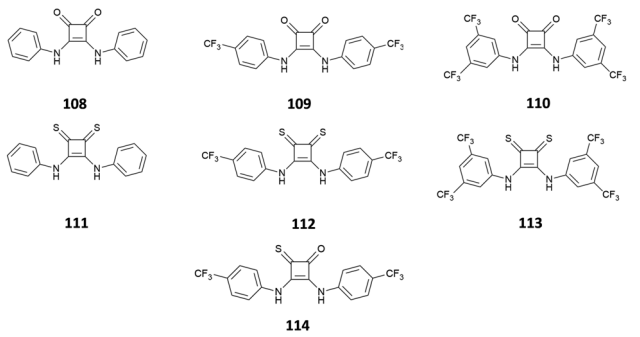

Fig. 38 Squaramides **108–114** studied by Gale and co-workers.

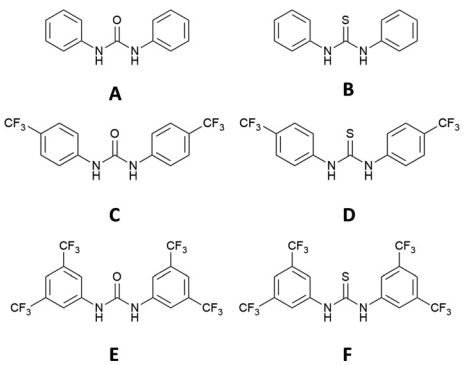

Fig. 39 Ureas and thioureas used in anion transport studies in comparison with the analogous squaramides **108–114**.

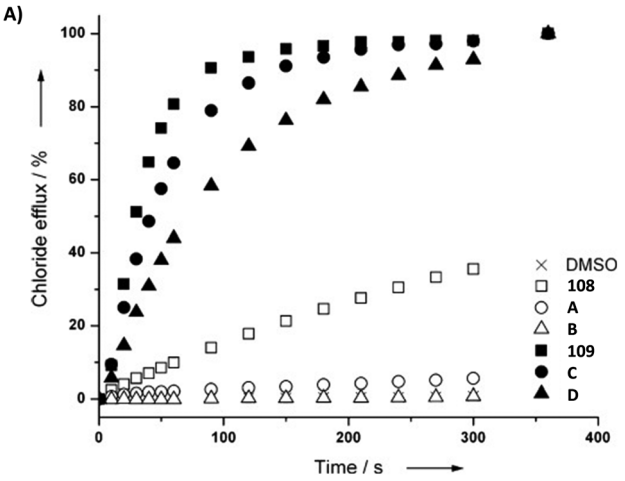

B)

Compound	Ka [M^{-1}]	EC_{50} [mol %]	n	Log P
108	260	1.38	1.7	2.02
A	15	ND	ND	3.66
B	31	ND	ND	2.51
109	458	0.06	1.2	3.87
C	43	0.22	1.6	5.50
D	75	0.42	2.2	4.35
110	643	0.01	1.1	5.71
E	41	0.16	2.0	7.34
F	88	0.30	1.4	6.20

Fig. 40 Chloride efflux promoted by **108** and **109** and their analogous urea and thiourea (**A–B** and **C–D** for **108** and **109**, respectively) at a concentration of 1 mol% (receptor to lipid) from unilamellar POPC vesicles loaded with 489 mM NaCl solution buffered to pH 7.2 with 5 mM sodium phosphate salts and dispersed in 489 mM $NaNO_3$ solution buffered to pH 7.2 with 5 mM sodium phosphate salts (A). Summary of the chloride association constants (K_{ass}) and anion transport data obtained through Hill analysis (EC_{50} and n), and calculated log P of **108–110** and their analogous ureas and thioureas **A–F** (B). Reproduced with the permission from ref. 93. Copyright Wiley 2012 (Fig. 1).

Most likely, the explanation for the superior transport abilities of the squaramide systems **108–110** in comparison to their urea and thiourea analogues is the enhanced anion-binding properties of the former.

In a subsequent study, Gale and co-workers proposed another family of fluorinated squaramide-derivatives **115–119** (Fig. 41) able to induce caspase mediated cell death.[94] In particular, also **109** was able to disrupt autophagy by HCl symport, while the apoptosis of the HeLa and A549 cancer cells was caused by the concomitant transport of Cl^- and Na^+.

Based on these results obtained on squaramides, Gale, Jolliffe and co-workers considered also the use of thiosquaramides **111–113** for anion binding and transport.[95] The antiport Cl^-/NO_3^- assay conducted on unilamellar POPC vesicles loaded with 489 mM NaCl solution buffered to pH 7.2 with 5 mM sodium phosphate salts and dispersed in 489 mM $NaNO_3$ solution buffered to pH 7.2 with 5 mM sodium phosphate salts evidenced the scarce anion transport ability of **111–113** at this pH. However, the spectrophotometric determination of the pK_a suggested that at pH 7.2 thiosquaramides considered are in their deprotonated form, thus characterized by a negative

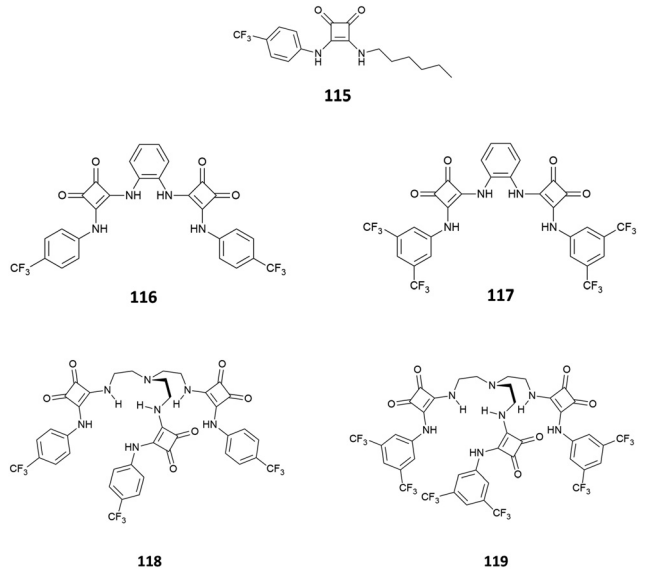

Fig. 41 Fluorinated squaramides **115–119** able to cause cancer cells death.

charge and not able to bind and transport chloride species across to the membrane (pK_a = 7.3, 5.3, and 4.9 for 111, 112, and 113, respectively). The transport assay repeated at pH 4.0 of the vesicles internal and external buffered solutions, highlighted how under these experimental conditions the anion transport ability of thiosquaramides **111–112** switched on, due to the presence of the compounds in their neutral form, demonstrating a strong pH-dependence of their anion transport properties. This experimental evidence is further supported by the value of the EC_{50} calculated through the Hill analysis, which pointed out that oxosquaramides **108–110** are potentially potent anion transporters at both pH 7.2 and 4.0, the analogous thiosquaramide **111** is unable to do transport at pH 7.2 and can be switched on at pH 4.0, whereas the anion transport properties of **112** dramatically increased at lower pH values. It is worthy noting that **113** is unable to transport the anion species at pH 4.0 probably due to its too high lipophilicity (see Table 1).

Finally, the same group decided to investigate the anion binding and transport properties of a mixed oxothiosquaramide **114**,[96] based on the results previously obtained and reported above that allowed them to identify in the oxo- and thio-squaramide bearing the *p*-trifluoromethylphenyl group as the substituent in the symmetric structure the best anion transporters through synthetic membranes. Indeed, authors first reported the anion binding properties of **114** towards Cl^- (as TBA salt) by means of ^{1}H-NMR in DMSO-d_6/0.5%H_2O, which pointed out an association constant for the formation of the host–guest adduct similar to that calculated for the analogous oxosquaramide. Interestingly, the value of the pK_a of **114** was found to be close to that calculated for the analogous thiosquaramide **112**. For this reason, to investigate the anion transport properties of **114**, a series of experiments were conducted at pH values of 7.2 and 4.0. The results indicated that, as already observed in the case of the analogous thiosquaramide, **114** possessed a higher anion transport ability at pH 4.0. In this case also, the value of the EC_{50} calculated through the Hill analysis of the data supported the experimental trend.

After the first results obtained on oxo-, thio-, and oxothiosquramides, the effect in Cl^- binding and transport of the presence of additional H-bond donor groups in the molecular skeleton of the transporters was investigated.

Caltagirone and co-workers described the ability of bisindolylsquaramide **21** (see the Anion binding section) to bind and transport chloride.[84] It was demonstrated that **21** was able to bind chloride with 10-fold higher association constant than the analogous urea (K_{ass} = 1200 and 128 M^{-1} in DMSO-d_6/0.5%H_2O for **21** and the analogous urea, respectively) and that it was able to efficiently transport this anion across the synthetic phospholipidic membrane with EC_{50} = 0.12 mol%. Starting from these results, the same group in collaboration with Quesada demonstrated that the combination of the indolyl and the 3,5-trifluoromethylphenyl substituents on the molecular skeleton of squaramide **120** (Fig. 42) allowed in obtaining the transport efficiency results similar to those obtained for the symmetric squaramide **110** in the Cl^-/NO_3^- antiport assay, and slightly better in the Cl^-/HCO_3^- exchange assay.[97]

The authors concluded that the simultaneous presence of the indolyl group and the electro-withdrawing 3,5-trifluoromethylphenyl group confers an ideal lipophilicity to the system. In the same study, Caltagirone and co-workers proposed the first simple numerical model to fit and analyse the experimental data of Cl^- transport. Based on these preliminary results, Scorciapino and co-workers proposed an extended version of this theoretical model taking into account the impact of several important parameters on the transport efficiency of the anionophore, such as the equilibrium in the formation of the adduct, the balance between the affinity of the transporter towards chloride and the lipophilicity of the anionophore, and the effect of the diffusivity of the carrier and its complex

Table 1 Summary of the anion transport of **108–113** at pH values of 4.0 and 72

Compound	EC_{50} [mol%] at pH 7.2	EC_{50} [mol%] at pH 4.0
108	1.38	1.42
109	0.06	0.08
110	0.01	0.01
111	ND[a]	0.0125
112	0.68	0.0125
113	ND[a]	ND[a]

[a] Not enough active to calculate an EC_{50} value.

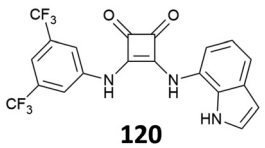

Fig. 42 Non-symmetric squaramide **120** bearing indolyl and 3,5-trifluoromethylphenyl substituents.

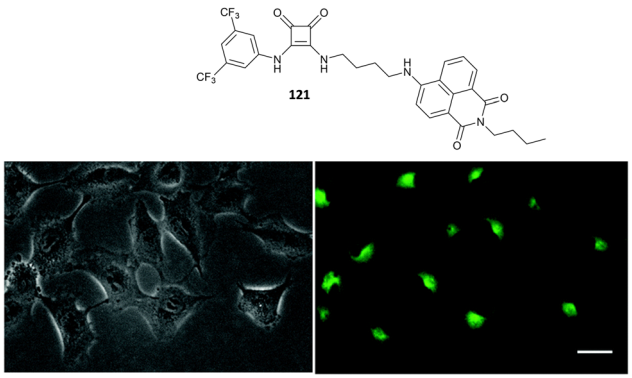

Fig. 43 Bright field (left) and fluorescence images (right) of A549 cells after 24 hours incubation with **121** (1.0 μM). Adapted from ref. 101. Copyright RSC 2018.

through the membrane.[98] It is worthy to highlight that *in silico* investigation and quantitative structure–activity relationship (QSAR) analysis were previously proposed to better understand and predict the anion transport properties of this type of simple squaramides.[99,100]

A similar non-symmetric squaramide **121** (Fig. 43) was reported by Gale and co-workers.[101] This system was able to transport Cl^- with an IC_{50} of 0.15 from a Cl^-/NO_3^- exchange assay. In this case, the presence of the 1,8-naphthalimide fluorophore also allows compound **121** to be used for fluorescence imaging in cells, with high efficiency in staining of living A549 cells (Fig. 43).

Davis, Gale and co-workers have highlighted that an appropriate balance between the affinity for Cl^- and the transport efficiency should be considered when designing anionophores. Indeed, steroidal squaramides **122–127** express excellent chloride binding properties (K_{ass} in the range 10^6–10^9 M^{-1} in water-saturated

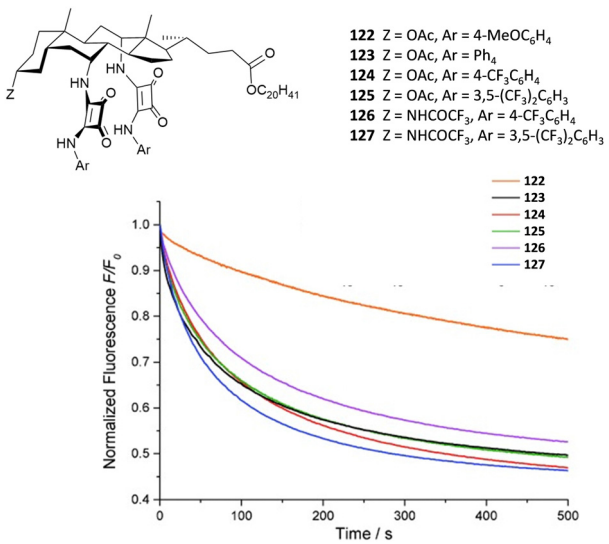

Fig. 44 Steroidal squaramides **122–127** and lucigenin assay for the Cl^-/NO_3^- exchange by **121–126**. Reproduced with permission from ref. 102. Copyright Wiley 2015.

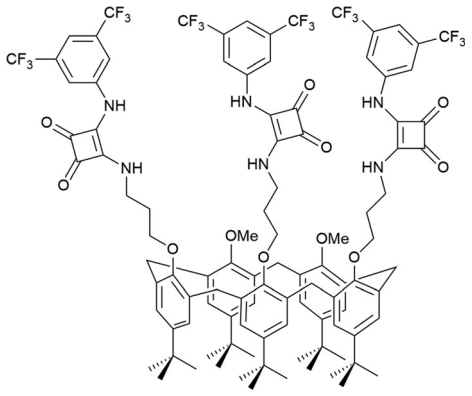

128

Fig. 45 Tris-squaramide **128**.

$CHCl_3$) but negligible transport activity (Fig. 44 for Cl^-/NO_3^- exchange in large unilammelar vesicles).[102]

Very recently, Elmes and co-workers have described the moderate transport properties of amidosquaramides which can be switched on at acidic pH as shown above for thiosquaramides.[103]

Valkenier and co-workers described a calix[6]arene functionalised with three squaramide groups **128** (Fig. 45) which is

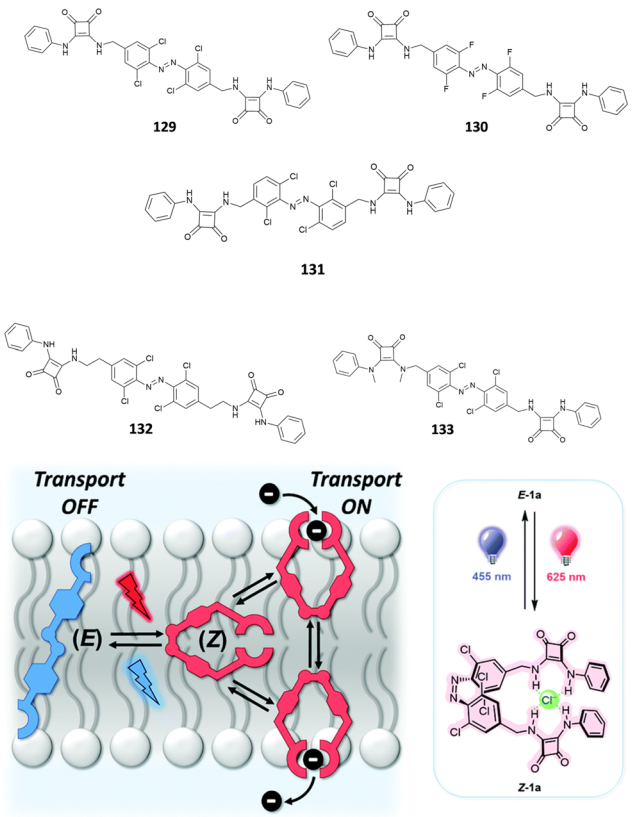

Fig. 46 Photo-switchable squaramides **129–133** and cartoon illustrating their ON–OFF transport abilities. Reproduced with permission from ref. 105. Copyright RSC 2021.

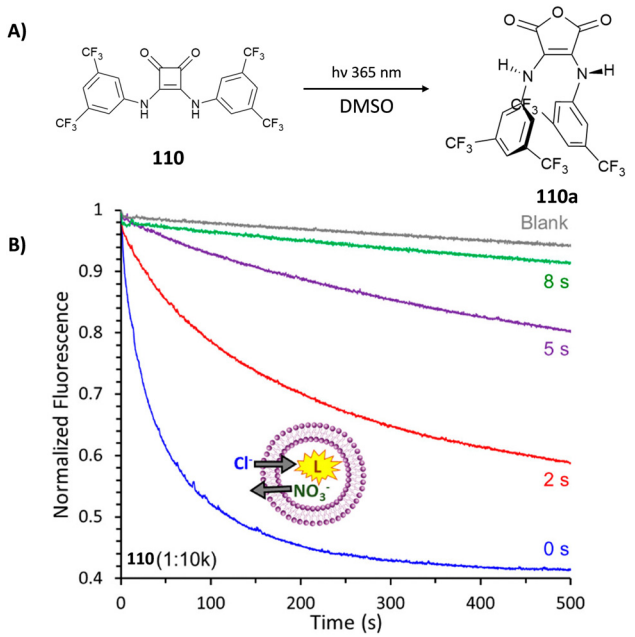

Fig. 47 Photo-conversion of **110** to **110a** upon irradiation in DMSO (A). Evidence of efficiency loss in Cl^- transport upon different irradiation times studied by the lucigenin assay (B). Reproduced with permission from ref. 106. Copyright ACS 2023.

able to efficiently transport Cl^-, NO_3^-, HCO_3^-, and AcO^- as demonstrated by HPTS and lucigenin fluorescence assays. This represents a rare example of a tris-squaramide as an active anion transporter.[104]

Recently, Langton and co-workers have shown a very elegant example of a photo-switchable azobenzene family (**129–133**) functionalised with squaramide substituents which can switch ON and OFF their chloride transport ability (Fig. 46).[105] Indeed, by using the HPTS-assay, the authors showed that the *Z* isomers were able to transport chloride with an EC_{50} 8-fold higher than the *E* isomer (EC_{50} = 0.07 mol% and EC_{50} = 0.58 mol% for *Z* and *E*, respectively for compound **128**). This difference was attributed to a change in the mobility in the membrane as well as to chloride encapsulation.

Another example of transport modulation by light was recently reported by Costa, Rotger and co-workers.[106] As shown in Fig. 47(A), upon irradiation at 365 nm, squaramide **110** was photo-converted to maleic anhydride **110a** which is not able to act as chloride transporter as demonstrated by the lucigenin assay. When large unilamellar POPC vesicles were irradiated in the presence of **110**, a loss in the transport efficiency was observed during time due to the photo-conversion (Fig. 47(B)).

Conclusions

In this review, we have highlighted the versatility of the squaramide H-bonding motif in the design of receptors for anions with different functions. The results reported in the literature so far corroborate the excellent properties of this class of compounds in the anion binding, sensing, and extraction, and in the transmembrane anion transport. While simple bis-substituted squaramides have been successfully employed for anion transmembrane transport, macrocyclic and acyclic systems featuring two or more squaramide moieties in their structures appear more versatile for anion binding, sensing, and extraction, in particular in the case of sulfate and phosphate tetrahedral anions. However, solubility issues have, in most of the cases, prevented the application of squaramide systems in real matrices. For this reason, particular attention in the future design of squaramide receptors should be given to the functionalisation with polar groups for increasing the solubility, possibly in water.

In terms of fluorescence responses, the results reported in the literature suggest that the direct conjugation of fluorogenic fragments to the squaramide central core in most cases hampers the optical properties of the systems. On the other hand, the introduction of an alkyl or more flexible spacer seems to facilitate the fluorescence emission. It is interesting to note that, to the best of our knowledge, in terms of optical sensing, squaramides have never been employed in the development of arrays for anion recognition.

Moreover, the fundamental parameters such as the affinity for the anion species, binding modes, acid–base equilibrium, and lipophilicity of the system must be carefully balanced when designing an anionophore. On the other hand, the higher the affinity towards the anion species, the more efficient the anion binding and sensing properties of the receptor. Despite the low number of examples reported so far, squaramides have been demonstrated to be useful synthons in the construction of interlocked systems such as rotaxanes and their ability to be photoconverted or to be linked in photo-switchable molecules is opening novel strategies for the development of more sophisticated and stimuli-responsive materials. In particular, the possibility to act as both the H-bond acceptor and donor favours the self-assembly of squaramides to form complex architectures for the development of supramolecular gels which can be used for remediation or sensing applications or for the development of MOFs in the presence of metal ions for anion recognition.

We believe that in the next few years we will assist to an increasing interest towards this class of molecules.

Author contributions

All authors contributed equally to this review.

Conflicts of interest

There are no conflicts to declare.

Acknowledgements

R. M. acknowledges Ms E. Palazzetti for valuable advice in producing the graphical content. The authors thank the Italian Ministero dell'Università e della Ricerca (MIUR) (PRIN_PNRR

P2022XHLTX), and NextGeneration EU, Return project (PE0000005 CUP:F53C22000730002) for financial support.

Notes and references

1 S. Cohen and S. G. Cohen, *J. Am. Chem. Soc.*, 1966, **88**, 1533–1536.
2 D. Quiñonero, C. Garau, A. Frontera, P. Ballester, A. Costa and P. M. Deyà, *Chem. – Eur. J.*, 2002, **8**, 433–438.
3 V. E. Zwicker, K. K. Y. Yuen, D. G. Smith, J. Ho, L. Qin, P. Turner and K. A. Jolliffe, *Chem. – Eur. J.*, 2018, **24**, 1140–1150.
4 J. Alemán, A. Parra, H. Jiang and K. A. Jørgensen, *Chem. – Eur. J.*, 2011, **17**, 6890–6899.
5 V. Amendola, G. Bergamaschi, M. Boiocchi, L. Fabbrizzi and M. Milani, *Chem. – Eur. J.*, 2010, **16**, 4368–4380.
6 V. Amendola, L. Fabbrizzi, L. Mosca and F.-P. Schmidtchen, *Chem. – Eur. J.*, 2011, **17**, 5972–5981.
7 P. Lach, A. Garcia-Cruz, F. Canfarotta, A. Groves, J. Kalecki, D. Korol, P. Borowicz, K. Nikiforow, M. Cieplak, W. Kutner, S. A. Piletsky and P. S. Sharma, *Biosens. Bioelectron.*, 2023, **236**, 115381.
8 A. Rostami, C. J. Wei, G. Guérin and M. S. Taylor, *Angew. Chem., Int. Ed.*, 2011, **50**, 2059–2062.
9 S.-J. Choi, B. Yoon, J. D. Ray, A. Netchaev, L. C. Moores and T. M. Swager, *Adv. Funct. Mater.*, 2020, **30**, 1907087.
10 D. Wu, R. Jiang, L. Luo, Z. He and J. You, *Inorg. Chem. Front.*, 2016, **3**, 1597–1603.
11 S. Mommer and S. J. Wezenberg, *ACS Appl. Mater. Interfaces*, 2022, **14**, 43711–43718.
12 X.-J. Cai, Z. Li and W.-H. Chen, *Mini-Rev. Org. Chem.*, 2018, **15**, 148–156.
13 R. Ian Storer, C. Aciro and L. H. Jones, *Chem. Soc. Rev.*, 2011, **40**, 2330–2346.
14 L. A. Marchetti, L. K. Kumawat, N. Mao, J. C. Stephens and R. B. P. Elmes, *Chem*, 2019, **5**, 1398–1485.
15 R. Prohens, S. Tomàs, J. Morey, P. M. Deyà, P. Ballester and A. Costa, *Tetrahedron Lett.*, 1998, **39**, 1063–1066.
16 R. Prohens, M. C. Rotger, M. N. Piña, P. M. Deyà, J. Morey, P. Ballester and A. Costa, *Tetrahedron Lett.*, 2001, **42**, 4933–4936.
17 M. H. Al-Sayah and N. R. Branda, *Thermochim. Acta*, 2010, **503–504**, 28–32.
18 A. Grundzi, S. A. Healy, O. Fenelon and R. B. P. Elmes, *Res. Chem.*, 2022, **4**, 100652.
19 G. Picci, M. C. Aragoni, M. Arca, C. Caltagirone, M. Formica, V. Fusi, L. Giorgi, F. Ingargiola, V. Lippolis, E. Macedi, L. Mancini, L. Mummolo and L. Prodi, *Org. Biomol. Chem.*, 2023, **21**, 2968–2975.
20 G. Picci, S. Farotto, J. Milia, C. Caltagirone, V. Lippolis, M. C. Aragoni, C. Di Natale, R. Paolesse and L. Lvova, *ACS Sens.*, 2023, **8**, 3225–3239.
21 L. K. Kumawat, C. Wynne, E. Cappello, P. Fisher, L. E. Brennan, A. Strofaldi, J. J. McManus, C. S. Hawes, K. A. Jolliffe, T. Gunnlaugsson and R. B. P. Elmes, *ChemPlusChem*, 2021, **86**, 1058–1068.
22 C. V. Esteves, J. Costa, D. Esteban-Gómez, P. Lamosa, H. Bernard, C. Platas-Iglesias, R. Tripier and R. Delgado, *Dalton Trans.*, 2019, **48**, 10104–10115.
23 G. Ambrosi, M. Formica, V. Fusi, L. Giorgi, E. Macedi, M. Micheloni, P. Paoli, R. Pontellini and P. Rossi, *Chem. – Eur. J.*, 2011, **17**, 1670–1682.
24 J. H. Yang and S. K. Kim, *Chem. Commun.*, 2023, **59**, 9988–9991.
25 J. L. Sessler, *Anion Receptor Chemistry*, Royal Society of Chemistry, Cambridge, 2016.
26 I. Ravikumar and P. Ghosh, *Chem. Soc. Rev.*, 2012, **41**, 3077–3098.
27 S. H. Murch, T. T. MacDonald, J. A. Walker-Smith, P. Lionetti, M. Levin and N. J. Klein, *Lancet*, 1993, **341**, 711–714.
28 A. V. Nieuw Amerongen, J. G. M. Bolscher, E. Bloemena and E. C. I. Veerman, *Biol. Chem.*, 1998, **379**, 1–18.
29 A. B. Olomu, C. R. Vickers, R. H. Waring, D. Clements, C. Babbs, T. W. Warnes and E. Elias, *N. Engl. J. Med.*, 1988, **318**, 1089–1092.
30 R. Custelcean and B. A. Moyer, *Eur. J. Inorg. Chem.*, 2007, 1321–1340.
31 J. W. Pflugrath and F. A. Quiocho, *Nature*, 1985, **314**, 257–260.
32 B. L. Jacobson and F. A. Quiocho, *J. Mol. Biol.*, 1988, **204**, 783–787.
33 Z. Rodriguez-Docampo, E. Eugenieva-Ilieva, C. Reyheller, A. M. Belenguer, S. Kubik and S. Otto, *Chem. Commun.*, 2011, **47**, 9798–9800.
34 K. M. Mullen and P. D. Beer, *Chem. Soc. Rev.*, 2009, **38**, 1701–1713.
35 R. Custelcean, *Chem. Commun.*, 2013, **49**, 2173–2182.
36 A. Pramanik, B. Thompson, T. Hayes, K. Tucker, D. R. Powell, P. V. Bonnesen, E. D. Ellis, K. S. Lee, H. Yu and M. A. Hossain, *Org. Biomol. Chem.*, 2011, **9**, 4444–4447.
37 C. Raposo, M. Almaraz, M. Martín, V. Weinrich, M. L. Mussóns, V. Alcázar, M. C. Caballero and J. R. Morán, *Chem. Lett.*, 1995, 759–760.
38 C. Jin, M. Zhang, L. Wu, Y. Guan, Y. Pan, J. Jiang, C. Lin and L. Wang, *Chem. Commun.*, 2013, **49**, 2025–2027.
39 Y. Liu, Y. Qin and D. Jiang, *Analyst*, 2015, **140**, 5317–5323.
40 L. Qin, S. J. N. Vervuurt, R. B. P. Elmes, S. N. Berry, N. Proschogo and K. A. Jolliffe, *Chem. Sci.*, 2020, **11**, 201–207.
41 L. Qin, J. R. Wright, J. D. E. Lane, S. N. Berry, R. B. P. Elmes and K. A. Jolliffe, *Chem. Commun.*, 2019, **55**, 12312–12315.
42 L. Qin, A. Hartley, P. Turner, R. B. P. Elmes and K. A. Jolliffe, *Chem. Sci.*, 2016, **7**, 4563–4572.
43 R. B. P. Elmes, K. K. Y. Yuen and K. A. Jolliffe, *Chem. – Eur. J.*, 2014, **20**, 7373–7380.
44 R. B. P. Elmes and K. A. Jolliffe, *Supramol. Chem.*, 2015, **27**, 321–328.
45 N. A. Tzioumis, K. K. Y. Yuen and K. A. Jolliffe, *Supramol. Chem.*, 2018, **30**, 667–673.
46 J. D. E. Lane, W. J. H. Greenwood, V. W. Day, K. A. Jolliffe, K. Bowman-James and L. Adriaenssens, *New J. Chem.*, 2022, **46**, 18119–18123.

47 V. Ramalingam, M. E. Domaradzki, S. Jang and R. S. Muthyala, *Org. Lett.*, 2008, **10**, 3315–3318.
48 L. Fan, T. Xu, J. Feng, Z. Ji, L. Li, X. Shi, C. Tian and Y. Qin, *Electroanalysis*, 2020, **32**, 805–811.
49 J. Beswick, V. Blanco, G. De Bo, D. A. Leigh, U. Lewandowska, B. Lewandowski and K. Mishiro, *Chem. Sci.*, 2015, **6**, 140–143.
50 A. Arun, A. Docker, H. Min Tay and P. D. Beer, *Chem. – Eur. J.*, 2023, **29**, e202301446.
51 R. L. Spicer, C. C. Shearman and N. H. Evans, *Chem. – Eur. J.*, 2023, **29**, e202203502.
52 D. Jagleniec, Ł. Dobrzycki, M. Karbarz and J. Romański, *Chem. Sci.*, 2019, **10**, 9542–9547.
53 D. Jagleniec, S. Siennicka, Ł. Dobrzycki, M. Karbarz and J. Romański, *Inorg. Chem.*, 2018, **57**, 12941–12952.
54 D. Jagleniec, N. Walczak, Ł. Dobrzycki and J. Romański, *Int. J. Mol. Sci.*, 2021, **22**, 10754.
55 D. Jagleniec, M. Wilczek and J. Romański, *Molecules*, 2021, **26**, 2751.
56 M. Zaleskaya, Ł. Dobrzycki and J. Romański, *Int. J. Mol. Sci.*, 2020, **21**, 9465.
57 M. Zaleskaya, M. Karbarz, M. Wilczek, Ł. Dobrzycki and J. Romański, *Inorg. Chem.*, 2020, **59**, 13749–13759.
58 M. Zaleskaya-Hernik, Ł. Dobrzycki and J. Romański, *Int. J. Mol. Sci.*, 2023, **24**, 8536.
59 M. Zaleskaya-Hernik, E. Megiel and J. Romański, *J. Mol. Liq.*, 2022, **361**, 119600.
60 S. Zdanowski, P. Piątek and J. Romański, *New J. Chem.*, 2016, **40**, 7190–7196.
61 P. Manesiotis, A. Riley and B. Bollen, *J. Mater. Chem. C*, 2014, **2**, 8990–8995.
62 S. Cavalera, F. Di Nardo, G. Spano, L. Anfossi, P. Manesiotis and C. Baggiani, *Anal. Methods*, 2020, **12**, 5729–5736.
63 J. D. E. Lane, G. Shiels, P. Ramamurthi, M. Müllner and K. A. Jolliffe, *Macromol. Rapid Commun.*, 2023, 2300406.
64 J. Huang, Y. Shi, G.-z Huang, S. Huang, J. Zheng, J. Xu, F. Zhu and G. Ouyang, *Angew. Chem., Int. Ed.*, 2022, **61**, e202206749.
65 A. C. Sedgwick, J. T. Brewster, T. Wu, X. Feng, S. D. Bull, X. Qian, J. L. Sessler, T. D. James, E. V. Anslyn and X. Sun, *Chem. Soc. Rev.*, 2021, **50**, 9–38.
66 M. Neus Piña, M. Carmen Rotger, A. Costa, P. Ballester and P. M. Deyà, *Tetrahedron Lett.*, 2004, **45**, 3749–3752.
67 M. N. Piña, B. Soberats, C. Rotger, P. Ballester, P. M. Deyà and A. Costa, *New J. Chem.*, 2008, **32**, 1919–1923.
68 R. Prohens, G. Martorell, P. Ballester and A. Costa, *Chem. Commun.*, 2001, 1456–1457.
69 E. Delgado-Pinar, C. Rotger, A. Costa, M. N. Piña, H. R. Jiménez, J. Alarcón and E. García-España, *Chem. Commun.*, 2012, **48**, 2609–2611.
70 K. A. López, M. N. Piña and J. Morey, *Sens. Actuators, B*, 2013, **181**, 267–273.
71 A. Frontera, J. Morey, A. Oliver, M. N. Piña, D. Quiñonero, A. Costa, P. Ballester, P. M. Deyà and E. V. Anslyn, *J. Org. Chem.*, 2006, **71**, 7185–7195.
72 R. B. P. Elmes, P. Turner and K. A. Jolliffe, *Org. Lett.*, 2013, **15**, 5638–5641.
73 R. P. Orenha, V. B. da Silva, G. F. Caramori, F. S. de Souza Schneider, M. J. Piotrowski, J. Contreras-Garcia, C. Cardenas, M. Briese Gonçalves, F. Mendizabal and R. L. T. Parreira, *New J. Chem.*, 2020, **44**, 17831–17839.
74 R. P. Orenha, V. B. da Silva, G. F. Caramori, M. J. Piotrowski, G. R. Nagurniak and R. L. T. Parreira, *Phys. Chem. Chem. Phys.*, 2021, **23**, 11455–11465.
75 C. B. Black, B. Andrioletti, A. C. Try, C. Ruiperez and J. L. Sessler, *J. Am. Chem. Soc.*, 1999, **121**, 10438–10439.
76 M. Boiocchi, L. Del Boca, D. E. Gómez, L. Fabbrizzi, M. Licchelli and E. Monzani, *J. Am. Chem. Soc.*, 2004, **126**, 16507–16514.
77 T. Gunnlaugsson, M. Glynn, G. M. Tocci, P. E. Kruger and F. M. Pfeffer, *Coord. Chem. Rev.*, 2006, **250**, 3094–3117.
78 A. A. Abogunrin, S. A. Healy, O. Fenelon and R. B. P. Elmes, *Chemistry*, 2022, **4**, 1288–1299.
79 C. Jin, M. Zhang, C. Deng, Y. Guan, J. Gong, D. Zhu, Y. Pan, J. Jiang and L. Wang, *Tetrahedron Lett.*, 2013, **54**, 796–801.
80 H. Niu, Q. Shu, S. Jin, B. Li, J. Zhu, L. Li and S. Chen, *Spectrochim. Acta, Part A*, 2016, **153**, 194–198.
81 A. Rostami, A. Colin, X. Y. Li, M. G. Chudzinski, A. J. Lough and M. S. Taylor, *J. Org. Chem.*, 2010, **75**, 3983–3992.
82 J. D. E. Lane and K. A. Jolliffe, *Org. Biomol. Chem.*, 2023, **21**, 3226–3234.
83 G. Picci, J. Milia, M. C. Aragoni, M. Arca, S. J. Coles, A. Garau, V. Lippolis, R. Montis, J. B. Orton and C. Caltagirone, *Molecules*, 2021, **26**, 1301.
84 G. Picci, M. Kubicki, A. Garau, V. Lippolis, R. Mocci, A. Porcheddu, R. Quesada, P. C. Ricci, M. A. Scorciapino and C. Caltagirone, *Chem. Commun.*, 2020, **56**, 11066–11069.
85 M. Zaleskaya, D. Jagleniec and J. Romański, *Dalton Trans.*, 2021, **50**, 3904–3915.
86 M. Zaleskaya-Hernik, Ł. Dobrzycki, M. Karbarz and J. Romański, *Int. J. Mol. Sci.*, 2021, **22**, 13396.
87 M. Zaleskaya, D. Jagleniec, M. Karbarz, Ł. Dobrzycki and J. Romański, *Inorg. Chem. Front.*, 2020, **7**, 972–983.
88 M. Porel, V. Ramalingam, M. E. Domaradzki, V. G. Young, V. Ramamurthy and R. S. Muthyala, *Chem. Commun.*, 2013, **49**, 1633–1635.
89 A. Danao, V. Ramalingam, V. Ramamurthy and R. S. Muthyala, *J. Photochem. Photobiol., A*, 2017, **344**, 108–113.
90 Y. Hong, J. W. Y. Lam and B. Z. Tang, *Chem. Soc. Rev.*, 2011, **40**, 5361–5388.
91 D. Zhai, W. Xu, L. Zhang and Y.-T. Chang, *Chem. Soc. Rev.*, 2014, **43**, 2402–2411.
92 L. K. Kumawat, A. A. Abogunrin, M. Kickham, J. Pardeshi, O. Fenelon, M. Schroeder and R. B. P. Elmes, *Front. Chem.*, 2019, **7**, 354.
93 N. Busschaert, I. L. Kirby, S. Young, S. J. Coles, P. N. Horton, M. E. Light and P. A. Gale, *Angew. Chem., Int. Ed.*, 2012, **51**, 4426–4430.
94 N. Busschaert, S.-H. Park, K.-H. Baek, Y. P. Choi, J. Park, E. N. W. Howe, J. R. Hiscock, L. E. Karagiannidis,

I. Marques, V. Félix, W. Namkung, J. L. Sessler, P. A. Gale and I. Shin, *Nat. Chem.*, 2017, **9**, 667–675.

95 N. Busschaert, R. B. P. Elmes, D. D. Czech, X. Wu, I. L. Kirby, E. M. Peck, K. D. Hendzel, S. K. Shaw, B. Chan, B. D. Smith, K. A. Jolliffe and P. A. Gale, *Chem. Sci.*, 2014, **5**, 3617–3626.

96 R. B. P. Elmes, N. Busschaert, D. D. Czech, P. A. Gale and K. A. Jolliffe, *Chem. Commun.*, 2015, **51**, 10107–10110.

97 G. Picci, I. Carreira-Barral, D. Alonso-Carrillo, C. Busonera, J. Milia, R. Quesada and C. Caltagirone, *Org. Biomol. Chem.*, 2022, **20**, 7981–7986.

98 M. A. Scorciapino, G. Picci, R. Quesada, V. Lippolis and C. Caltagirone, *Membranes*, 2022, **12**, 292.

99 N. Busschaert, S. J. Bradberry, M. Wenzel, C. J. E. Haynes, J. R. Hiscock, I. L. Kirby, L. E. Karagiannidis, S. J. Moore, N. J. Wells, J. Herniman, G. J. Langley, P. N. Horton, M. E. Light, I. Marques, P. J. Costa, V. Félix, J. G. Frey and P. A. Gale, *Chem. Sci.*, 2013, **4**, 3036–3045.

100 I. Marques, P. M. R. Costa, M. Q. Miranda, N. Busschaert, E. N. W. Howe, H. J. Clarke, C. J. E. Haynes, I. L. Kirby, A. M. Rodilla, R. Pérez-Tomás, P. A. Gale and V. Félix, *Phys. Chem. Chem. Phys.*, 2018, **20**, 20796–20811.

101 X. Bao, X. Wu, S. N. Berry, E. N. W. Howe, Y.-T. Chang and P. A. Gale, *Chem. Commun.*, 2018, **54**, 1363–1366.

102 S. J. Edwards, H. Valkenier, N. Busschaert, P. A. Gale and A. P. Davis, *Angew. Chem., Int. Ed.*, 2015, **54**, 4592–4596.

103 L. A. Marchetti, T. Krämer and R. B. P. Elmes, *Org. Biomol. Chem.*, 2022, **20**, 7056–7066.

104 A. Singh, A. Torres-Huerta, T. Vanderlinden, N. Renier, L. Martínez-Crespo, N. Tumanov, J. Wouters, K. Bartik, I. Jabin and H. Valkenier, *Chem. Commun.*, 2022, **58**, 6255–6258.

105 A. Kerckhoffs, Z. Bo, S. E. Penty, F. Duarte and M. J. Langton, *Org. Biomol. Chem.*, 2021, **19**, 9058–9067.

106 M. Vega, L. Martínez-Crespo, M. Barceló-Oliver, C. Rotger and A. Costa, *Org. Lett.*, 2023, **25**, 3423–3428.